AMÉLIE BUREL

Numerical implementation of a non-linear constitutive equations for hydrogels

Thesis report of Master Erasmus Mundus in Computational Mechanics

...

5/11/2009

Supervisors: Steven Le Corre and Erwan Verron

Table of Contents

Introduction

When a network of long polymers is immersed in a suitable solvent, it can swell forming a polymeric gel. This interesting property is exploited in diverse technologies such as medical devices, drug delivery and actuators. Recent advances have been made to propose new constitutive equations devoted to polymeric gels (Hong et al. 2008a). These constitutive equations imply non-linear hyperelastic solid behaviours coupled to the migration of small molecules into the network. They are founded on the general theory of poroelasticity with liquid transport, the difficulty being due to the introduction of large strain.

The aim of my Master thesis was to first get familiar with the theory of Hong et al. (2008a) and the previous general theories about polymeric gels then, as the main objective, was to implement the constitutive model of Hong et al. (2008a) in a finite element code (COMSOL Multiphysics) and solve various test cases.

This report explains the different steps of my Master thesis. The first chapter describes the properties and applications of polymeric gels as well as the general theories about them. The model of Hong et al. (2008a) is explained in the second chapter which also contains the analytical resolution of two simple test cases. The third chapter describes the procedure of the implementation of the previous model in COMSOL Multiphysics. The results of two test cases are presented in the following chapter. Finally, the results and failures of the implementation are analysed and improvements are suggested.

Chapter 1 : Background

I. DEFINITION OF HYDROGELS AND APPLICATIONS

A. Definition of hydrogel

A polymeric gel is an aggregate formed by a swollen elastomer after immersion into a solvent. The gel is called a hydrogel when the solvent is water. Figure 1 illustrates the swelling of a piece of elastomer.

The elastomer is a three dimensional network of long cross-linked polymers. The long flexible chains of polymer can accept large chain deformations. At the scale of the sample, the elastomeric network is capable of large and reversible (elastic) deformations. Moreover, the cross-links prevent the polymer molecules from dissolving within the solvent. In the hydrogel case, the polymers are water-insoluble and hydrophilic.

The solvent is a species of molecules with low molecular weight. These molecules can migrate into the network of long polymers.

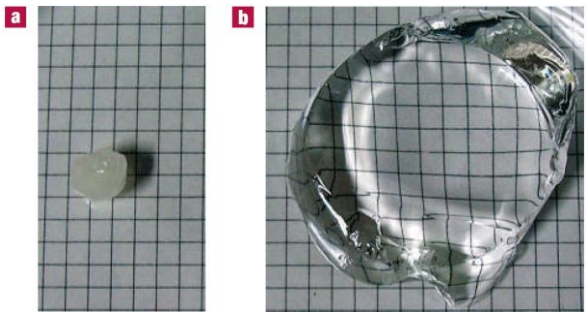

Figure 1. (a) Elastomer, (b) Swollen elastomer

B. Properties of hydrogels

Polymeric gels can experience reversible abrupt volume changes: hydrogels can contain 99% of water. When the small molecules migrate in, the elastomer can swell and hold a large amount of solvent while maintaining its structure. Reversibly, it can shrink while releasing the small molecules of solvent. This mechanism is shown in figure 2.

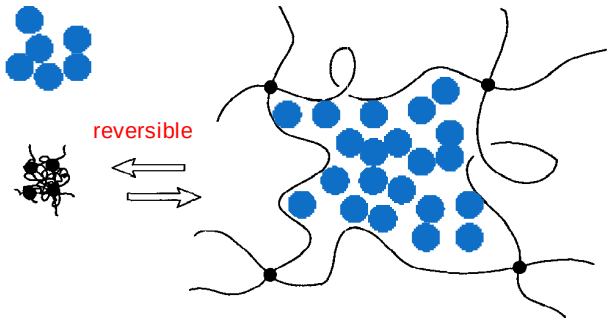

Figure 2. Mechanism of swelling/shrinking of the polymeric gel

Polymeric gels are environmentally sensitive. As reviewed in the online discussion of the mechanics of gels led by Qi (2007), such gels swell/shrink in response to various environmental stimuli such as relatively small changes of temperatures, pH values, electric signals or light. For example, the negatively thermoresponsive hydrogels shrinks as the temperature increases because hydrophobic interactions become strengthened above a critical temperature. In this report, the mechanism studied will be only the chemically induced swelling and the shrinking under a mechanical load (with a constant chemical potential).

Polymeric gels have two interesting properties: the elasticity of the network and the fluidity of the solvent. The elasticity comes from the strong bonds cross-linking the long polymers. On the other hand, as the polymers and solvent molecules are aggregated by weak bonds, the small molecules can easily change neighbours and migrate in the same way as in a liquid. The elasticity and the migration are coupled: the accumulation of solvent brings about the network's swelling whereas the solvent migrates in response to the deformation of the network.

C. Applications

Polymeric gels have various applications at the microscale: the actuation times are on the order of milliseconds at this scale. As diffusion phenomena exist in the polymeric gels, the actuation times will be quite long at the bigger scales.

Polymeric gels are used in diverse medical devices including microgel drug carriers/ pumps, scaffolds in reparation of human tissues, biosensors which respond to specific molecules (glucose or antigens for example), contact lenses and medical electrodes. Figure 3 shows an example of drug carrier: this gel can shrink wrapping the drug. An overview of state-of-the-art environment-sensitive hydrogels for drug delivery is provided in the articles Qiu and Park (2001) and Bromberg and Ron (1998).

Figure 3. . Drug delivery with a bioresponsive hydrogel

The presentation of Suo (2008) and the gel article on wikipedia review some other applications of polymeric gel: autonomous microfluidic actuators, sustained-release delivery systems, disposable diapers, dressings for healing of burn, breast implants and granules for holding soil moisture in arid areas. Figure 4 illustrates one example of these devices: the micro valves used in fluidics.

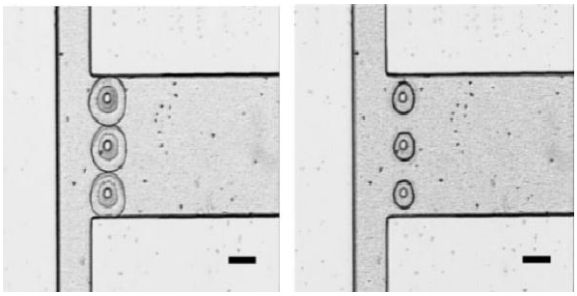

Figure 4. Valves in fluidics

II. STATE OF THE ART IN THE MECHANICAL MODELLING

A. Driving mechanisms

As reviewed in the online discussion of the mechanics of gels led by Qi (2007), the mechanism of swelling/shrinking of the polymeric gels is explained by the competition between two kinds of interactions: polymer-polymer macromolecules and polymer-solution macromolecules. This corresponds to two molecular processes involved in the free energy: the stretching/contraction of the network and the mixing of the network with the small molecules.

These processes are mainly driven by entropic forces. When the network swells, the polymer chains are deformed and an elastic retractive force develops. Since the extended configuration is less probable for the chains, their deformations yield a decrease in the entropy. The equilibrium is reached when these opposing forces are balanced. The competition between these processes and associated forces is controlled through environmental stimuli.

Thus, polymeric gels are a complex system coupling mass transport (diffusion) and large deformation, controlled by multiple thermodynamic forces. The mechanical mechanisms include relaxation effects related to the viscoelastic behaviour of polymers. The relative time scale of diffusion is linked with the mutual diffusion process. These two processes imply a complex rate for the diffusion in polymers.

As explained in Hong et al. (2008), polymeric gels allow two modes of large deformation: one local and one “global”, as shown on figure 5. First the small molecules can rearrange locally quickly. This implies a change of shape but not volume. Then the small molecules can have slow long-range migrations. In this case, the polymeric gel changes both shape and volume as shown on the following figure. The speed of the device swelling/shrinking is related to the characteristic time of this slow diffusion which depends on the size of the sample.

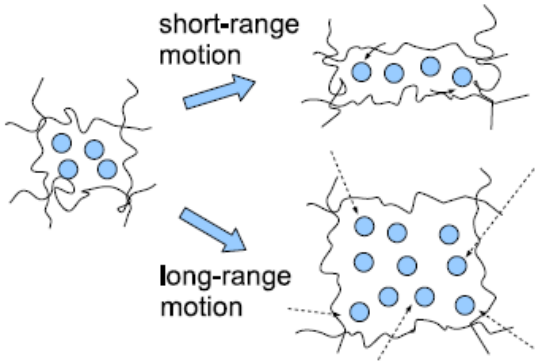

Figure 5. The two modes of deformation for the gel

B. Challenges

Polymeric gel is a complex system with interesting properties and promising applications. In many of hydrogel-based devices using their property of volume change, time should be accurately controlled knowing the variations of the environmental conditions. Therefore high fidelity constitutive models

are required for the swelling/shrinking process. Moreover, the models should be suitable for numerical methods, such as finite element methods.

Numerical investigations have been carried out however (though or although are better choices) most use simple theoretical cases far removed from some complex devices. For example, better models for the hydrogel damage should be developed because it is important to the design many hydrogel-based devices such as medical devices. The online discussion of the mechanics of gels led by Qi (2007) raises other problems with the modelling of polymeric gels.

C. State of the art of hydrogel modelling

1. Poroelasticity

Many studies have been carried out on the mass transport (flow of fluid) in an elastic solid with connected pores such as sponge, soil, living tissues, crystal and elastomer network. This subject is known as diffusion in elastic solids, or elasticity of fluid-infiltrated porous solids, or poroelasticity.

First, Gibbs (1878) expressed a thermodynamic theory of large deformation of an elastic solid which absorbs a fluid. It assumed that the solid and the fluid have reached the equilibrium. Then, Biot (1941) combined a similar thermodynamic theory with Darcy's law to model the motion of the fluid in a fluid-filled porous elastic material. He used the theoretical model of a coherent solid skeleton and a freely moving pore fluid.

Other works on poroelasticity are explained in Detournay and Cheng (1993). For example, poroelasticity was used to analyse compaction of soils, deformation of tissues, studies about bones, diffusion of atoms and swelling of hydrogels. An example of more advanced poroelasticity is the kinetic theory of Tanaka et al. (1979) and Tanaka and Fillmore (1973) which involves the friction between the polymers and solvent molecules as a limiting factor for the swelling of a gel.

2. Flory-Huggins constitutive equations

Horkay and Mc Kenna (2007) proposed a review on the modelling consideration for equilibrium swelling/shrinking behaviours of polymeric gels. It reminds the basic thermodynamic considerations of rubber elasticity and swelling using existing network models and a continuum point of view. This help to understand the Flory-Huggins constitutive equations which is generally used to describe the behaviour of polymeric gels.

In the survey of the behaviour of a swollen elastomeric network, two features should be considered:

- The original nature of the polymeric network in the undiluted state: formulation of the Helmoltz free energy of the network using the phenomenological theories of rubber elasticity and the molecular statistical models which provide the phenomenological behaviour of the dry network
- The specific behaviour of the swollen network using similar ideas: formulation of the mixing free energy as a function of the swelling ratio added to the elastic free energy

a) Elastic free energy of the dry rubber

First, the dry elastomer is studied and an expression of elastic Helmoltz free energy will be determined.

(1) Continuum description

The continuum description of rubber-like materials is based on the Finite Elasticity Theory. This uses the stretch ratio in each direction λ_i defined as $\lambda_i = l_{current}/l_{initial}$. The Valanis-landel Strain Energy Density Function $W(\lambda_1, \lambda_2, \lambda_3)$ is used as it describes well the mechanical response of crosslinked rubber and several statistical mechanical models are shown in this form. W is the mechanical part of the Helmoltz Free Energy. Valanis and Landel made the assumption that W is a separable function of the stretches λ_i:

$$W(\lambda_1,\lambda_2,\lambda_3) = w(\lambda_1) + w(\lambda_2) + w(\lambda_3) + a\ ln(\lambda_1 \lambda_2 \lambda_3) \quad \textbf{(1)}$$

The term $a\ \ln(\lambda_1 \lambda_2 \lambda_3)$ is zero for the polymeric network in the undilute state with the incompressibility assumption but can be important when the network swells. However some molecular models also include this term.

Two common Valanis-Landel forms are the Neo-Hookean and the Mooney-Rivlin forms. Several molecular models use the Neo-Hookean form even if dry rubbers do not have a Neo-Hookean behaviour.

(2) Statistical characteristics of polymer networks

Several structural parameters are used to characterise the ideal polymer network. The real network will be considered by reference to the parameters of the perfect network as they always present defects. Explicit expressions for the relation between the molecular structure and the elastic properties are determined using statistical models.

The most important structural parameters of a network are the concentration of elastic chains or that of elastically active junctions connecting the macromolecules.

(3) Network models

Statistical theories and simplified network models allow formulating an equation of state for the polymeric network which permits any deformation including swelling.

Molecular models express the way how the stress influences the conformational distribution of a polymeric assembly chains. Then predictive relationships will be derived to relate the molecular structure and topology of the polymeric network to the macroscopic behaviour as the swelling.

Classically, the theories of rubber elasticity are based on the two following assumptions:

1) The total elastic free energy of the network is derived by summing the elastic free energy of the single network chains, thus ignoring the energy contribution and the deformation state dependency of the interaction between chains.
2) The end-to-end distribution of the chains constructing the network follows a Gaussian curve.

Various models exist to derive the network behaviour from the statistical properties of the individual polymer molecules. The more common are the following ones:

- *The Affine Model*

The basic assumption of the affine model is the linear transformation (affinity) of the mean position of the junctions and the end-to-end vectors in the macroscopic strain.
The elastic free energy is expressed by:

$$\Delta F_{el}^{aff} = kT\left[\frac{\nu_{el}}{2V_0}(\lambda_1^2+\lambda_2^2+\lambda_3^2-3)-\frac{\mu_{el}}{V_0}\ln(\lambda_1\lambda_2\lambda_3)\right] \quad \textbf{(2)}$$

where ν_{el} is the number of the elastic chains and μ_{el} is the number of junctions in the network

- *The Phantom Model*

The basic assumption of the phantom model is the free movements of a polymer chain through another one. Every network junctions oscillates around its mean position.
The elastic free energy is expressed by:

$$\Delta F_{el}^{ph} = kT\left[\frac{\xi}{2V_0}(\lambda_1^2+\lambda_2^2+\lambda_3^2-3)\right] \quad \textbf{(3)}$$

where ξ is the cycle rank, i.e., the number of independent circuits in the network considered

- *The constrained Junction Fluctuation Model*

The two previous models cannot perfectly describe the real network behaviour because they are two limiting cases. Another model is necessary to span the behaviour between the phantom and the affine models. The model proposed by Ronca and Allegra (1975) and Flory (1977) uses the assumptions of constrained fluctuations and affine deformation of fluctuation domains. More details can be found in the Hoknay and Mc Kenna (2007).

b) Mixing contribution to the free energy

When the polymer network is swollen, there is an additional term in the free energy due to the mixing. The thermodynamic of this process is controlled by the interaction between the polymer and the small molecules. As there is no explicit molecular model for the crosslinked polymer solution, the functional dependence of the free energy of the mixing is generally assumed to be the same in a swollen network as in a polymer solution. The thermodynamics of polymer solutions can be described with two methods:

- The classical mean-field theories such as the Flory-Huggins model described below
- The asymptotic scaling theories which use an analogy between polymer chain statistics and critical phenomenon and consider correlations between monomers.
  A description of these theories can be found in the Horkay and McKenna (2007)

The Flory-Huggins model is build using statistics and a lattice model as described in Kausch et al. (2001). First the free energy of molecular mixing ΔF_m is given by*:*

$$\Delta F_m = \Delta H_m - T\,\Delta S_m \quad \textbf{(4)}$$

where ΔH_m is the enthalpy and ΔS_m is the entropy. The two components of the free energy are detailed below.

(1) Entropy of mixing

The entropy of mixing can be obtained using a lattice model showing the mixing of two kinds of small molecules: N_1 molecules of first type and N_2 of the second one. The lattice contains $N_0=N_1+N_2$

sites with one molecule per site as sketched on Figure 6 (a). The Boltzmann law (and the Stirling approximation) gives the following expression for the change of entropy:

$$\Delta S_m = -R(\phi_1 \ln \phi_1 + \phi_2 \ln \phi_2) \quad \textbf{(5)}$$

with $n_i=N_i/N_0$ and $\Phi_i=n_i/(n_1+n_2)$ is the volume ratio of molecules of type i

Then the second species is taken as a polymer: the small molecules are connected together, which limits the number of possible "arrangements". If N2 chains with x segments and N1 small molecules of type 1 are considered, there are $N_0=N_1+xN_2$ sites in total. Figure 6 (b) sketches an example of lattice with x=10. The computation of the mixing entropy of such a system is explained in the Appendix 2.9 of Kausch et al. (2001). The final expression is given by:

$$\Delta S_m = -R\left(\phi_1 \ln \phi_1 + \frac{\phi_2}{x} \ln \phi_2\right) \quad \textbf{(6)}$$

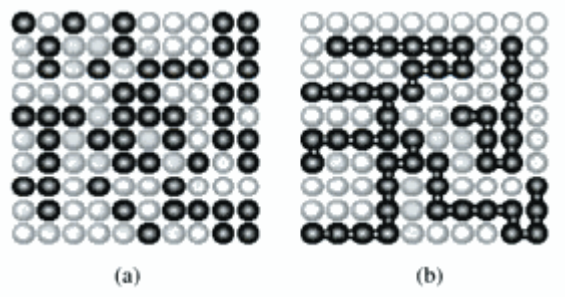

Figure 6. Lattice model for the mixing of two molecule species
(a) with two kinds of small molecules (b) with small molecules and chains of 10 segments

(2) Enthalpy of mixing

As explained in Kausch et al. (2001), there are different contacts in a binary mixing of a polymer (1) in a solvent (2):

- Contacts (1,1) between segments of polymer
- Contacts (2,2) between molecules of the solvent
- Contacts (1,2) between segment of polymer and molecules of solvent

When the solvent molecules are mixed with the polymer, new pairs (1, 2) are created by dissociation of one pair of (1, 1) and one of (2, 2). The enthalpy of mixing is the sum of all the enthalpy of formation of these new pairs Δw_{12}. The parameter of interaction of Flory-Huggins is defined by:

$$\chi = \frac{z\Delta w_{12}}{kT} \quad \textbf{(7)}$$

where z is the number of coordination of the lattice.

The expression of the enthalpy of mixing (per mole of sites) is given by:

$$\Delta H_m = RT\chi\phi_1\phi_2 \quad \textbf{(8)}$$

The entropy and the enthalpy of mixing are replaced by their expression in the equation. Thus, the Flory-Huggins mixing free energy of a polymer solution is given by:

$$\Delta F_m = RT\left(\phi_1 \, ln\, \phi_1 + \frac{\phi_2}{x} ln\, \phi_2 + \chi \phi_1 \phi_2\right) \quad \textbf{(9)}$$

An alternative expression of the Flory-Huggins mixing free energy is:

$$\Delta F_{mix} = RT[n_1 \ln(1-\varphi) + n_2 \ln(\varphi) + \chi n_1 \varphi] \quad \textbf{(10)}$$

where φ is the volume fraction of the polymer, χ is the Flory-Huggins interaction parameter and n_1 and n_2 are the numbers of moles of solvent and polymer respectively.

c) Flory-Huggins constitutive equation

As reviewed in Horkay and McKenna (2007), the swelling of a cross-linked polymer network can be described by the Frenkel-Flory-Rehner theory. This theory developed in Flory and Rehner (1946) is based on the basic assumption that the elastic (ΔF_{el}) and mixing (ΔF_{mix}) contributions in the free energy that come with the swelling of the network are separable and additive. The total free energy of the network-solvent system ΔF is given by:

$$\Delta F = \Delta F_{el} + \Delta F_{mix} \quad \textbf{(11)}$$

Macroscopic swelling observations can be connected to the molecular network structure using this model. The experimental characterisation of swollen polymeric network is explained in Horkay and McKenna (2007).

3. Viscoelastic diffusion models

As explained previously, diffusion is an important phenomenon in the swelling/shrinking behaviour of the polymeric gels. The mass transport process which allows small solvent molecules to enter the polymeric network is very complex. No theoretical framework or mathematical model can explain properly this mechanism so far.

Three steps can be considered in the mass transport process. First small molecules are absorbed on the surface of the polymer network. Secondly, the solvent molecules diffuse through the polymeric material. Finally, the small molecules desorb on the downstream surface of the polymer.

These mass transport mechanisms are affected by various parameters such as the polymer structure, temperatures, mechanical deformation and solvent-polymer interaction. Plastificization has also a great influence: when the local solvent volume fraction becomes high enough, the polymer goes from a glassy state to a rubbery state. As the polymer chains can move in the rubbery state, they can readily rearrange to accommodate solvent molecules. Conversely, as polymers are hard and brittle in the glassy state, the diffusion becomes rather complex.

Several diffusion models exist to describe mass transport mechanisms. The simplest model is the Fickian or Case I diffusion with a flux J proportional to the gradient of concentration: $J = -\rho D \partial c / \partial x$. This model is based on the assumption that the surface concentration reachs its equilibrium value immediately after a change in conditions and stays constant during the sorption process.

However solvent-polymer systems do not generally follow this simple law and the modelling of transport mass depends on characteristic times of the system. Briefly, the diffusion has Fickian

behaviour if the characteristic diffusion time is much longer than the polymer relaxation time. Conversely, the diffusion process exhibits a Case-II behaviour while the characteristic diffusion time is much shorter than the polymer relaxation time. Finally, the diffusion process in the glassy polymer presents anomalous behaviour if the two characteristic times are close.

As it was first observed in 1946, some polymer-solvent systems exhibit sharp boundaries and this separation between swollen and dry polymer moves linearly with time, thus with a constant velocity. This was later called "Case II" diffusion.

All diffusion models have a mass uptake of the form $M=k\ t^n$ with t the time and k and n are constants. n is ½ in the Fickian diffusion, 1 in the Case II and between ½ and 1 for the anomalous diffusion.

In conclusion, mass transport in polymer networks has been described with various models whose explanations can be found in De Kee et al. (2005). In spite of various trials, no fine unified model which can take into account both Fickian and non-Fickian diffusions were generated so far. Nevertheless the question of the utility of such a model is still being considered. Maybe a diffusion model could be developed with the help of numerical method as suggested in the discussion about Mechanics of hydrogels submitted by Qi (2007).

4. Various other works

Here are presented some other works carried out on the mechanical behaviour of polymeric gels.

a) Study about the behaviour under tensile test/ compression

Gao (1999) proposes an explanation about the difference of gel behaviour between tensile test and compression. Indeed the elastic modulus under tension may be up to 1.6times of that under compression. Long polymeric chains can only uphold tensile force but not compression along chains, even under small deformations. This phenomenon is explained using a simplified 2D micromodel and constitutive models for elastic modulus are derived in the small strain case.

b) Shape of the network interface

Some papers propose modelling to predict the shape of the swollen networks. For example Dolbow et al. (2004, 2005) present two-phase model for chemically induced swelling in hydrogels. This continuum model allows sharp interface separating swollen and collapsed phases of the holding polymer network which agrees with experimental observations. Hybrid eXtended-Finite-Element/Level-Set Method are employed to find approximate solutions to the governing equations of the model. This is applied to the swelling of a spherical traction-free specimen in contact with a reservoir of uniform chemical potential in Dolbow et al. (2004). The new paper in 2005 provides improvement in this model and extension to multi-dimensional problems with applications such as unstable interfacial evolution in polymeric gels.

5. Conclusion

There are some other papers developing molecular or constitutive models for polymeric gels that we will not expand on in this report (such as Durning and Morman, 1993; Tsai et al., 2004).

Furthermore, many studies were also carried out about the experimental characterisations of polymeric gels and about various applications and devices making use of hydrogel properties.

In conclusion, various studies were carried out about coupling between mass transport and deformation in polymeric gels evoking different conceptual images. However nowadays these theoretical works cannot predict the experimental behaviour of complex devices because some are limited to small deformations or do not have numerical development such as finite elements.

This report will deal with a recent model proposed in Hong et al (2008a). This modelling of polymeric gels is explained in the next chapter.

Chapter 2 : Modelling

I. INTRODUCTION

As explained in the introduction, the goal of this project is to implement numerically a constitutive equation for hydrogels in a finite element code. The model implemented will be explained in this part. First, this model is presented in the article **A THEORY OF COUPLED DIFFUSION AND LARGE DEFORMATION IN POLYMERIC GELS** published in 2008 by Wei Hong, Xuanhe Zhao, Jinxiong Zhou and Zhigang Suo. This article formulates a monophasic theory of the coupled mass transport and large deformation for polymeric gels.

This field theory of gels uses first the nonequlibrium thermodynamics using a gel system subject to mechanical and chemical loads (a "weight" and a "pump") which gives an equation for the Helmholtz free energy. The individual solvent molecule and polymer are assumed incompressible, which is enforced using a Lagrangian multiplier. The free energy is expressed using the Flory-Huggins constitutive equation.

Secondly the paper proposes a modelling for kinetics. Two modes of deformation are distinguished: the short-range and the long-range motions. The local rearrangements are considered fast enough to have a local equilibrium. The long-range migrations are slow and their characteristic time depends on the size of the sample: it increases as the size grows. The solvent molecules are assumed to diffuse in the polymeric network. Then the time-dependency of these migrations are modelled using a kinetic law.

The model will be illustrated with the test case of the uniaxial creep of a gel layer.

II. THEORETICAL PART: EXPLANATIONS ABOUT THE MODEL

A. Thermodynamics equations

1. Presentation of the system

The considered system is a gel subject to mechanical and chemical loads modelled respectively by a "weight" and a "pump" as sketched on Figure 7. The "weight" imposes a force P, a displacement δl and a work $P\delta l$. The "pump" imposes a chemical potential μ of the solvent molecules, a variation of the number of small molecules δM (injected) and an associated work $\mu\delta M$.

The dry network under no mechanical load is chosen as reference state. Every point of this dry network is located with a coordinate X in the reference state.

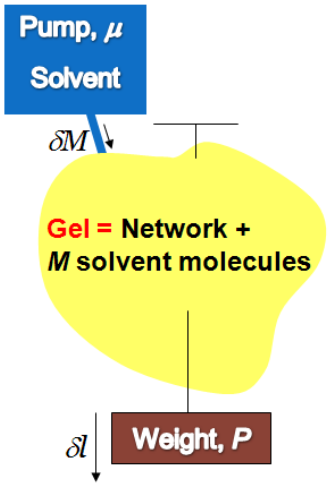

Figure 7. Gel subject to mechanical and chemical loads

The following assumptions are taken on this system:

- Equilibrium of the external solvent on its own
- Imaginary network of vanishing elastic stiffness in the external which allows to integrate on the full volume (gel and solvent) and on the interface areas between the gel and the external solvent

$dV(x)$ will be the element of volume and $N_K(X)dA(X)$ is an element of an interface with $dA(X)$ the area of the element and $N_K(X)$ the unit vector normal to the interface as shown on Figure 8.

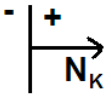

Figure 8. Direction of the unit normal vector

2. Mechanical equations

The point with a coordinate X moves to the coordinate *x(X,t)* in the current state at time t. The deformation gradient is given by:

$$F_{iK} = \frac{\partial x_i(X,t)}{\partial X_K} \qquad \textbf{(12)}$$

The gel is subject to mechanical forces: $B(X,t)\,dV$ in the volume and $T(X,t)\,dV$ on the interfaces.

The nominal stress $s_{iK}(X,t)$ is ruled by the classical partial differential equation of force balance given by the following equations.

$$\frac{\partial s_{iK}(X,t)}{\partial X_K} + B_i(X,t) = 0 \qquad in\ the\ volume \qquad \textbf{(13)}$$

$$\left(s_{iK}^{-}(X,t) - s_{iK}^{+}(X,t)\right)N_K(X,t) = T_i(X,t) \qquad on\ an\ interface \qquad \textbf{(14)}$$

The classical weak form can deduce using a continuous test function $\xi_i(X)$:

$$\int s_{iK}\frac{\partial \xi_i}{\partial X_K}dV = \int B_i\,\xi_i dV + \int T_i\,\xi_i dA \qquad \textbf{(15)}$$

The divergence theorem gives:

$$\int \frac{\partial (s_{iK}\xi_i)}{\partial X_K}dV = \int_{s^-} \xi_i s_{iK}^- N_K^- dA + \int_{s^+} \xi_i s_{iK}^+ N_K^+ dA = \int (s_{iK}^- - s_{iK}^+)\mathrm{N_K}\xi_i dA \qquad \textbf{(16)}$$

Therefore, the substitution of B_i and T_i by their expression in the equation 15 gives the equation 17.

$$\int s_{iK}\frac{\partial \xi_i}{\partial X_K}dV = \int (s_{iK}^- - s_{iK}^+)\mathrm{N_K}\xi_i dA - \int \xi_i \frac{\partial s_{iK}}{\partial X_K}dV \qquad \textbf{(17)}$$

3. Chemical equations

Solvent molecules at a chemical potential $\mu(X, t)$ are injected into the gel. The variables involved in this process are:

- $r(X,t)$: the number of molecules injected into the volume per unit time and volume
- $i(X,t)$: the number of molecules injected into an interface element per unit time and area
- $C(X,t)$: the nominal concentration of solvent molecules in a volume element (of dry polymer)
- $J_K(X,t)$: the flow of small molecules across an element of area

Assuming that there is no chemical reaction, the conservation equations are:

$$\frac{\partial \mathrm{C}(X,t)}{\partial \mathrm{t}} + \frac{\partial J_K(X,t)}{\partial X_K} = \mathrm{r(X,t)} \qquad in\ the\ volume \qquad \textbf{(18)}$$

$$\left(\mathrm{J_K^+}(X,t) - \mathrm{J_K^-}(X,t)\right)N_K(X,t) = \mathrm{i}(X,t) \qquad on\ an\ interface \qquad \textbf{(19)}$$

The application of divergence theorem on the flux gives:

$$\int \frac{\partial \mathrm{J}_K}{\partial X_K}dV = \int (J_K^- - J_K^+)\mathrm{N_K}dA \qquad \textbf{(20)}$$

Then the equations 19 and 20 are multiplied by an arbitrary test function ζ, integrated over the volume of the gel and the equation 13 is used. This gives the equation below.

$$\int \frac{\partial C}{\partial t}\zeta\, dV = \int J_K \frac{\partial \zeta}{\partial X_K}dV + \int r\zeta dV + \int i\zeta dA \qquad \textbf{(21)}$$

4. Nonequilibrium thermodynamics

The previous field equations will now be employed to write the structure of material laws, using nonequilibrium thermodynamics. If the markers move at a velocity δx/δt, the powers associated with the mechanical and chemical loads are respectively $\int B_i\,\delta x_i/\delta t\ dV + \int T_i\,\delta x_i/\delta t\ dA$ and $\int \mu r\, dV + \int \mu i\, dA$. The free-energy density is W in the current state. Hong et al. take the free energy

as a function of the deformation gardient F and the nominal concentration C. Then the small variation of the free-energy density is given by:

$$\delta W = \frac{\partial W(F,C)}{\partial F_{iK}}\delta F_{iK} + \frac{\partial W(F,C)}{\partial C}\delta C \quad \textbf{(22)}$$

The system presented above (gel+weight+pump) is considered as a thermodynamic system. Let G be the free energy of the system. G is the sum of free energy of the gel and the potential energy associated with the mechanical and chemical loads. Therefore, the rate of change of G is given by:

$$\frac{\delta G}{\delta t} = \int \frac{\delta W}{\delta t} dV - \int B_i \frac{\delta x_i}{\delta t}\ dV - \int T_i \frac{\delta x_i}{\delta t}\ dA - \int \mu r\, dV - \int \mu i\, dA \quad \textbf{(23)}$$

The use of equations 15, 18 and 22 gives:

$$\int B_i \frac{\delta x_i}{\delta t}\ dV + \int T_i \frac{\delta x_i}{\delta t}\ dA = \int s_{iK} \frac{\partial}{\partial X_K}\left(\frac{\delta x_i}{\delta t}\right) dV = \int s_{iK} \frac{\delta F_{iK}}{\delta t} dV \quad \textbf{(24)}$$

$$\frac{\delta W}{\delta t} = \frac{\partial W}{\partial F_{iK}}\frac{\delta F_{iK}}{\delta t} + \frac{\partial W}{\partial C}\left(r - \frac{\partial J_K(X,t)}{\partial X_K}\right) \quad \textbf{(25)}$$

The divergence theorem and the equation 20 are used on the flux:

$$\int \frac{\partial \mathrm{J}_K}{\partial X_K}\frac{\partial W}{\partial C} dV = \int \mathrm{J}_K \frac{\partial}{\partial X_K}\left(\frac{\partial W}{\partial C}\right) dV + \int \mathrm{i}\frac{\partial W}{\partial C} dA \quad \textbf{(26)}$$

Therefore the rate of change of G has the following expression:

$$\frac{\delta G}{\delta t} = \int \left(\frac{\partial W}{\partial F_{iK}} - s_{iK}\right)\frac{\delta F_{iK}}{\delta t} dV + \int \left(\frac{\partial W}{\partial C} - \mu\right) r\, dV + \int \left(\frac{\partial W}{\partial C} - \mu\right) i\, dA + \int \mathrm{J}_K \frac{\partial}{\partial X_K}\left(\frac{\partial W}{\partial C}\right) dV \quad \textbf{(27)}$$

According to the thermodynamic laws, the free energy of the system cannot increase i.e.:

$$\frac{\delta \mathrm{G}}{\delta \mathrm{t}} \leq 0 \quad \textbf{(28)}$$

This inequality must be verified for any r, i, J_k and $\delta x_i/\delta t$. Therefore each individual integral in equation 27 must either be negative or zero. Each integral in this equation corresponds to different processes of energy dissipation:

1) Local rearrangement of the solvent molecules

2 and 3) Injection of small molecules by the pumps

4) Long-range migration of the solvent molecules

As explained in the introduction, Hong et al. assume an instantaneous local rearrangement and a local equilibrium: the viscosity of the local rearrangement is neglected. Therefore the first integral of the equation 27 vanishes. This gives the following expression for the nominal stress:

$$s_{iK} = \frac{\partial W(F,C)}{\partial F_{iK}} \quad \textbf{(29)}$$

Hong et al. also assume a local equilibrium between the solvent molecules in every pump and those in the gel near the pump considered. Thus the second and the third integral of the equation 27 vanish. This gives the following expression for the chemical potential of the solvent molecules injected by the pump:

$$\mu = \frac{\partial W(F,C)}{\partial C} \quad \textbf{(30)}$$

Therefore, after the free energy function is fixed, the equations 29 and 30 provide the equations of state. As any constitutive equation in continuum mechanics, $W(F,C)$ should verify the assumption of objectivity: it should not change while the system is subject to a rigid-body motion. It is well known that this is equivalent to require that $W(F,C)$ is function of the deformation gradient only through $F_{iK}F_{iM}$.

5. Two limiting states

A mechanical load is suddenly applied to the polymeric gel and keeps constant after. There are two limiting states that can be analysed without looking at the diffusion mechanism of the small molecules. In the short-time limit, the small molecules have only time to rearrange locally but not to migrate. However the mechanical equilibrium ruled by equations 13, 14 and 29 has already been established.

In the long-time limit, both mechanical and chemical equilibrium have been reached. The free energy G of the system is minimum i.e. δG/δt =0. Therefore, the fourth integral of the equation 27 vanishes. Then, as the gel is in equilibrium with the external solvent, the chemical potential μ is homogeneous inside the gel and imposed by the external solvent. This boundary value problem is ruled by equations 13, 14, 29 and 30.

B. Molecular incompressibility

As the long polymers and solvent molecules can generally suffer large configurational variation without changing their volume, Hong et al. assume that these individual long polymers and solvent molecules are incompressible. Moreover, the polymeric gel should not contain void space. The condition of molecular incompressibility can be expressed as following:

$$det(F) = \frac{V_{total}}{V_{dry\ polymer}} = 1 + \frac{V_{small\ molecules}}{V_{dry\ polymer}} = 1 + \frac{V_{small\ molecules}}{N_{small\ molecules}} \frac{N_{small\ molecules}}{V_{dry\ polymer}} \quad \textbf{(31)}$$

Let ν be the volume per small molecule. As C is the nominal concentration, the previous expression becomes:

$$1 + \upsilon C = det(F) \quad \textbf{(32)}$$

This condition of molecular incompressibility can be enforced by a field of Lagrange multiplier $\Pi(X,t)$: the term $\alpha = \int \Pi(1 + \upsilon C - \det(F))dV$ is added to the free energy G of the system. Thus, there is the following new term in the equation 28:

$$\frac{\delta\alpha}{\delta t} = \int \frac{\delta\Pi}{\delta t}(1 + \upsilon C - det(F))dV + \int \Pi\left(\upsilon\frac{\delta C}{\delta t} - \frac{\partial}{\partial F_{iK}}(det(F))\frac{\delta F_{iK}}{\delta t}\right)dV \quad \textbf{(33)}$$

Let H_{iK} be the transpose of the inverse of F_{iK} i.e. $H_{iK}F_{iK} = \delta_{KL}$ and $H_{iK}F_{iK} = \delta_{KL}$. Then the following algebraic identity is used:

$$\frac{\partial\, det(F)}{\partial F_{iK}} = H_{iK} det\,(F) \quad \textbf{(34)}$$

Using this identity and the equation 22 with $\zeta = \Pi\upsilon$, the second integral β of the equation 34 becomes:

$$\beta = \int \Pi\upsilon r dV + \int \Pi\upsilon i dA + \int J_K \frac{\partial(\Pi\upsilon)}{\partial X_K} dV - \int \Pi\, H_{iK} det\,(F)\frac{\delta F_{iK}}{\delta t} dV \quad \textbf{(35)}$$

Therefore, the equations 30 and 31 become:

$$s_{iK} = \frac{\partial W(F,C)}{\partial F_{iK}} - \Pi \mathrm{H_{iK}}\ \det(\mathrm{F}) \quad \textbf{(36)}$$

$$\mu = \frac{\partial W(F,C)}{\partial C} + \Pi\upsilon \quad \textbf{(37)}$$

The Lagrangian multiplier Π can be interpreted as the osmotic pressure. When the solvent molecules move inside the polymeric network, the gel swells because of this pressure which goes against the elastic retractive force.

C. Free energy expression

An explicit expression of the free energy function *W(F,C)* is necessary to solve initial and boundary value problems. Hong et al. has chosen to express approximate behaviour of gels using the simplest form for W. Therefore, they use the Flory-Huggins constitutive equation described in the first chapter. As explained previously, the free energy function is composed of one term W_s coming from the stretching elasticity of the network and another W_m from the mixing of the polymers and solvent molecules:

$$W(F,C) = W_S(F) + W_m(C) \quad \textbf{(38)}$$

Hong et al. use the affine model described in the first chapter for the stretching contribution of the free energy function:

$$W_S(F) = \Delta F_{el}^{aff} = \frac{1}{2}kT\left[\frac{\nu_{el}}{V_0}(\lambda_1^2 + \lambda_2^2 + \lambda_3^2 - 3) - \frac{2\mu_{el}}{V_0}\log(\lambda_1\lambda_2\lambda_3)\right] \quad \textbf{(39)}$$

where λ_1, λ_2 and λ_3 are the three stretches, k is the Boltzmann's constant, V_0 is the volume of dry polymer, ν_{el} is the number of the elastic chains and μ_{el} is the number of junctions in the network. Let N be the number of elastic chains in the gel divided by the volume of the dry network V_0. Hong et al. assume the equality of ν_{el} and μ_{el}. Then the previous equation becomes:

$$W_S(F) = \frac{1}{2}NkT[\lambda_1^2 + \lambda_2^2 + \lambda_3^2 - 3 - 2\log(\lambda_1\lambda_2\lambda_3)] \quad \textbf{(40)}$$

The elastic free energy can also be expressed using the invariants of the right Cauchy-Green strain tensor $\mathbb{C} = F^T F$:

$$W_S(F) = \frac{1}{2} NkT[I_1 - 3 - \log(I_3)] \quad \textbf{(41)}$$

where I_1 is the first invariant ($I_1 = tr(\mathbb{C})$) and I_3 is the second invariant ($I_3 = det(\mathbb{C}) = (\lambda_1\lambda_2\lambda_3)^2$)

Let φ be the volume fraction of the polymer. The expression of φ is:

$$\varphi = \frac{V_{dry\ polymer}}{V_{total}} = \frac{1}{1 + \upsilon C} \quad \textbf{(42)}$$

Hong et al. use for $W_m(C)$ the Flory-Huggins mixing free energy described in the first chapter. Using the expression of φ, the equation 9 becomes:

$$W_m(C) = -\frac{kT}{\upsilon}\left[\upsilon C \log\left(1 + \frac{1}{\upsilon C}\right) + \frac{\chi}{1 + \upsilon C}\right] \quad \textbf{(43)}$$

where χ is the Flory-Huggins interaction parameter.

If s_1, s_2 and s_3 are the three principal nominal stresses, the equation 35 becomes:

$$s_1 = \frac{\partial W_s(F)}{\partial \lambda_1} - \Pi\lambda_1^{-1}\lambda_1\lambda_2\lambda_3 = NkT(\lambda_1 - \lambda_1^{-1}) - \Pi\lambda_2\lambda_3 \quad \textbf{(44)}$$

$$s_2 = NkT(\lambda_2 - \lambda_2^{-1}) - \Pi\lambda_1\lambda_3 \quad \textbf{(45)}$$

$$s_3 = NkT(\lambda_3 - \lambda_3^{-1}) - \Pi\lambda_1\lambda_2 \quad \textbf{(46)}$$

The expression 36 of the chemical potential becomes:

$$\mu = \frac{\partial W_m(C)}{\partial C} + \Pi\upsilon = kT\left[log\left(\frac{\upsilon C}{1 + \upsilon C}\right) + \frac{1}{1 + \upsilon C} + \frac{\chi}{(1 + \upsilon C)^2}\right] + \Pi\upsilon \quad \textbf{(47)}$$

The equations 42 to 45 are the equations of state for the model gel.

D. Kinetic law

Hong et al. model the long range migration of solvent molecules like a time-dependent process. In the equation 26, the fourth integrand should be negative definite for any flux. Therefore Hong et al. model the flow with a kinetic law as common practise:

$$J_K = -M_{KL}\frac{\partial \mu(X,t)}{\partial X_L} \quad \textbf{(48)}$$

where M_{KL} is the mobility: a symmetric positive-definite tensor. Like the free energy function, the mobility tensor depends on the deformation gradient F and the concentration C.

As well as the free energy function, the mobility tensor should follow the objectivity assumption. Therefore, $M_{KL}(F, C)$ should depend on the deformation gradient only through $F_{iK}F_{iM}$.

Finally, as a mean to develop the kinetic law, Hong et al. assume that the solvent molecules diffuse in the gel. As seen in the first chapter, diffusion is a common way to model the migration of small molecules into a polymeric network. Hong et al. use the simplest model of diffusion: they assume that the coefficient of diffusion D is isotropic and independent of the deformation gradient F and the concentration C. This assumption is only acceptable for the swollen gels where the ratio of solvent molecules is high. The diffusion is defined using $c(X,t)$ the true concentration of small molecules in

the current state, $j_i(X,t)$ the true flux of solvent molecules per unit area per unit time and $\mu(X,t)$ the chemical potential. Hong et al. use the following well-known expression for the true flux described for example in Feynman et al. 1963:

$$j_i = -\frac{cD}{kT}\frac{\partial \mu}{\partial x_i} \quad \textbf{(49)}$$

This expression is written in true quantity. Therefore Hong et al. convert it into an expression with nominal concentration and flow. The true concentration is defined as:

$$c = \frac{N_{solvent\ molecules}}{V_{total}} = \frac{N_{solvent\ molecules}}{V_{dry\ polymer} det\ (F)} = \frac{C}{det\ (F)} \quad \textbf{(50)}$$

The deformation of a material element of area $N_K dA$ in the reference state is $n_i da$ in the current state. These two quantities are related by the identity $det(F)\, F^{-T} dA\vec{N} = da\vec{n}$ i.e. $det(F) N_K dA = F_{iK} n_i da$. The number of molecules crossing a unit area per unit time can be written in true or nominal quantities:

$$j_i n_i da = J_K N_K dA \quad \textbf{(51)}$$

Therefore, the true and nominal fluxes are related by:

$$j_i = \frac{F_{iK}}{\det\,(F)} J_K \quad \textbf{(52)}$$

Then, the derivative of the chemical potential can be written as following:

$$\frac{\partial \mu}{\partial X_K} = \frac{\partial \mu}{\partial x_i}\frac{\partial x_i}{\partial X_K} = \frac{\partial \mu}{\partial x_i} F_{iK} \quad \textbf{(53)}$$

Combining the equations 50 and 51 and reminding the equation 48 gives:

$$j_i = -\frac{F_{iK}}{\det\,(F)} M_{KL}\frac{\partial \mu}{\partial x_i} F_{iL} = -\frac{cD}{kT}\frac{\partial \mu}{\partial x_i} \quad \textbf{(54)}$$

Using the definition of $H_{iK}$and the equation 49, the mobility tensor becomes:

$$M_{KL} = H_{iK} F_{iK} H_{iL} F_{iL} M_{KL} = \frac{cD}{kT}\frac{H_{iK} H_{iL}}{\det\,(F)} = \frac{CD}{kT} H_{iK} H_{iL} \quad \textbf{(55)}$$

Using the molecular incompressibility, the coefficient of diffusion can be written as:

$$M_{KL} = \frac{D}{\upsilon kT} H_{iK} H_{iL} [\det(F) - 1] \quad \textbf{(56)}$$

This mobility tensor defined with nominal quantities is anisotropic for large deformations.

The mobility tensor proposed by Hong et al. uses the assumption of self-diffusion of the solvent molecules. Therefore, this model may be wrong in case of prevailing macroscopic flow or convection of solvent molecules inside the polymeric gel.

The equation 47 gives the flux J_K as a function of the gradient of the chemical potential μ. The nominal flux can also be expressed as a function of the gradient of nominal concentration C using the chain rule of partial derivative:

$$J_K = -M_{KL}\frac{\partial \mu(F,C)}{\partial X_L} = -M_{KL}\frac{\partial \mu(F,C)}{\partial C}\frac{\partial C}{\partial X_L} = -D_{KL}\frac{\partial C}{\partial X_L} \quad \textbf{(57)}$$

The derivative expression 46 for the chemical potential (F,C) is:

$$\frac{\partial \mu}{\partial C} = \frac{kT\upsilon}{(1+\upsilon C)^2}\left[\frac{1}{\upsilon C} - \frac{2\chi}{1+\upsilon C}\right] \quad \textbf{(58)}$$

Using the equations 55 and 57 and the molecular incompressibility, the expression of D_{KL} becomes:

$$D_{KL} = \frac{D}{(1+\upsilon C)^2}\left[1 - \frac{2\chi\upsilon C}{1+\upsilon C}\right] H_{iK}H_{iL} \quad \textbf{(59)}$$

Using the kinetic laws 47 and 56 the equation of conservation 18 can be written in two ways:

$$\frac{\partial \mathrm{C}(X,t)}{\partial \mathrm{t}} - \frac{\partial}{\partial X_K}\left(M_{KL}\frac{\partial \mu(X,t)}{\partial X_L}\right) = \mathrm{r(X,t)} \quad \textbf{(60)}$$

$$\frac{\partial \mathrm{C}(X,t)}{\partial \mathrm{t}} - \frac{\partial}{\partial X_K}\left(D_{KL}\frac{\partial C(X,t)}{\partial X_L}\right) = \mathrm{r(X,t)} \quad \textbf{(61)}$$

E. Boundary conditions

In case of an initial value problem, the boundary conditions should be imposed at the interface between the gel and the external solvent. The chemical boundary condition can be either a prescribed chemical potential μ or an imposed flux i. For the mechanical boundary condition, either the position x or the traction T can be imposed.

Then, the constants of the equations must be estimated to solve numerically a problem using the presented model. Hong et al. uses the values of the literature for these constants. For example, for small-strain conditions, the dry cross-linked polymers have a shear modulus NkT of the order of $10^4 - 10^7 N/m^2$. Hong et al. remind that representative values of υ and kT are respectively $10^{-28}m^3$ and $4\times10^{-21}J$. Therefore, representative values of kT/υ and $N\upsilon$ are respectively $4\times10^7 Pa$ and $10^{-4} - 10^{-1}$. For the numerical applications in the next paragraphs, the value of $N\upsilon$ chosen will be 10^{-3}. The Flory-Huggins interaction parameter χ is worth between 0 and 1.2. As Hong et al. are interested in gels with large swelling ratios, they choose a low value of χ: 0.2.

Then, to estimate the value of the diffusion coefficient D, Hong et al. use the Stokes-Einstein formula $D = kT/(6\pi R\eta)$ which gives the coefficient of diffusion of a particle (much larger than a molecule) in a liquid. In the formula, R is the radius of a particle and η is the viscosity. Hong et al. estimate the coefficient of self-diffusion D at $8\times10^{-10}m^2/s$ considering water at room temperature: $R = 3\times10^{-10}m$ and $\eta = 0.89\times10^{-3}Pa.s$. If the characteristic size of the sample is L, the time scale will be L^2/D. For $L = 10^{-3}m$, the time scale will be $10^3 s$. All the chosen numerical values of the constants are summarised in the following table:

υ	kT	kT/ υ	NkT	N υ	χ	D
$10^{-28}m^3$	$4\times10^{-21}J$	$4\times10^7 Pa$	$10^4 - 10^7 N/m^2$	10^{-3}	0.2	$8\times10^{-10}m^2/s$

Table 1. Summary of the constant values

Remark: The value of NkT will be calculated according to the parameters of the numerical problem.

F. Summary of the equations to implement

- **Mechanical and chemical equations in the volume**

$$\frac{\partial s_{iK}(X,t)}{\partial X_K} + B_i(X,t) = 0 \qquad \textbf{(62)}$$

$$\begin{cases} \dfrac{\partial \mathrm{C}(X,t)}{\partial \mathrm{t}} - \dfrac{\partial}{\partial X_K}\left(M_{KL}\dfrac{\partial \mu(X,t)}{\partial X_L}\right) = \mathrm{r(X,t)} \quad \text{(a)} \\ \text{or} \\ \dfrac{\partial \mathrm{C}(X,t)}{\partial \mathrm{t}} - \dfrac{\partial}{\partial X_K}\left(D_{KL}\dfrac{\partial C(X,t)}{\partial X_L}\right) = \mathrm{r(X,t)} \quad \text{(b)} \end{cases} \qquad \textbf{(63)}$$

- **Boundary conditions**
  - *Chemical problem*: chemical potential μ or flux i are imposed on the boundary.
  - *Mechanical problem*: displacement x or traction T are imposed on the boundary.

- **Constitutive equations: expression of the free energy function**

$$W(F,C) = W_S(F) + W_m(C) \qquad \textbf{(64)}$$

$$\begin{cases} W_S(F) = \dfrac{1}{2}NkT[\lambda_1^2 + \lambda_2^2 + \lambda_3^2 - 3 - 2\log(\lambda_1\lambda_2\lambda_3)] \quad \text{(a)} \\ \text{or} \\ W_S(F) = \dfrac{1}{2}NkT[I_1 - 3 - \log(I_3)] \quad \text{(b)} \end{cases} \qquad \textbf{(65)}$$

$$W_m(C) = -\frac{kT}{\upsilon}\left[\upsilon C \log\left(1 + \frac{1}{\upsilon C}\right) + \frac{\chi}{1+\upsilon C}\right] \qquad \textbf{(66)}$$

- **Variables derived from the free energy function: stress s_{iK}, chemical potential μ and diffusion coefficients**

$$s_{iK} = \frac{\partial W(F,C)}{\partial F_{iK}} - \Pi \mathrm{H_{iK}} \det(\mathrm{F}) \qquad \textbf{(67)}$$

$$\mu = \frac{\partial W_m(C)}{\partial C} + \Pi\upsilon = kT\left[log\left(\frac{\upsilon C}{1+\upsilon C}\right) + \frac{1}{1+\upsilon C} + \frac{\chi}{(1+\upsilon C)^2}\right] + \Pi\upsilon \qquad \textbf{(68)}$$

$$\begin{cases} M_{KL} = \dfrac{D}{\upsilon kT} H_{iK}H_{iL}[\det(F) - 1] \qquad (a) \\ \text{or} \\ D_{KL} = \dfrac{D}{(1+\upsilon C)^2}\left[1 - \dfrac{2\chi\upsilon C}{1+\upsilon C}\right] H_{iK}H_{iL} \quad (b) \end{cases} \qquad \textbf{(69)}$$

III. TWO ANALYTICAL EXAMPLES

In their paper, Hong et al. implement their model by solving analytically the problem of the uniaxial creep of polymeric gel. This numerical example has also been studied by Zhang (2008). I have tried to find their results to this problem using Matlab software.

A. Free swelling

First a parallelepiped (cube or layer) of dry polymer of thickness L is immersed in a solvent with a chemical potential μ as sketched on the **Error! Reference source not found.**. The polymeric gel will well to equilibrate with the external solvent.

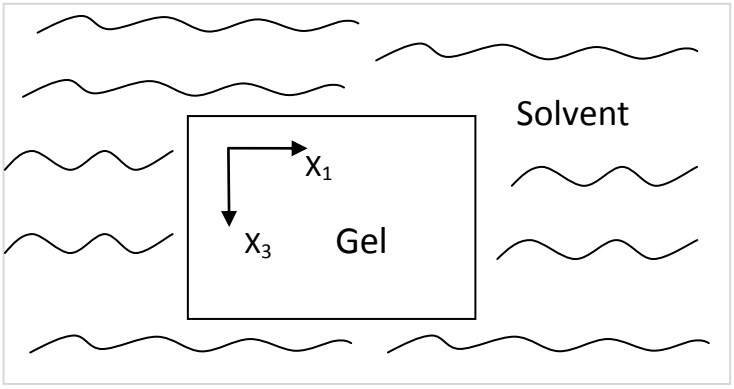

Figure 9. Gel immersed in a solvent

The gel is located with the coordinates X_1, X_2 and X_3 in the reference state as shown in the **Error! eference source not found.**. $x_i(X,t)$ are the coordinate of the marker in the current state. The stretches are defined as:

$$\lambda_i(X_i,t) = \frac{\partial x_i(X,t)}{\partial X_i} \quad \textbf{(70)}$$

As the gel swells under no constraint, the three stretches are the same: $\lambda_1 = \lambda_2 = \lambda_3$. Then, the chemical potential value is fixed at 0. Fixing s=0 and μ=0 in the equations 44 and 47 gives two expressions for the osmotic pressure Π:

$$\Pi = \frac{NkT}{\lambda_1^2}(\lambda_1 - \lambda_1^{-1}) = -\frac{kT}{\upsilon}\left[log\left(\frac{\upsilon C}{1+\upsilon C}\right) + \frac{1}{1+\upsilon C} + \frac{\chi}{(1+\upsilon C)^2}\right] \quad \textbf{(71)}$$

The condition of molecular incompressibility by:

$$\det(\mathrm{F}) = 1 + \upsilon C = \lambda_1\lambda_2\lambda_3 = \lambda_1^3 \quad \textbf{(72)}$$

This expression is inserted in equation 71. The rearrangement of this equation gives:

$$f(\lambda_1) = \frac{N\upsilon}{\lambda_1^2}(\lambda_1 - \lambda_1^{-1}) + log\left(1 - \frac{1}{\lambda_1^3}\right) + \frac{1}{\lambda_1^3} + \frac{\chi}{\lambda_1^6} = 0 \quad \textbf{(73)}$$

The root of this function is found using the Matlab function fzero (with 3 as initial guess): the equilibrium swelling ratio is $\lambda_1 = \lambda_2 = \lambda_3 = 3.215$. The Matlab program is in the appendix.

B. Uniaxial creep

1. Description of the uniaxial creep case

After swelling of a layer of polymer, this gel is fixed on a rigid substrate. As shown on Figure 10, a weight is applied on a permeable plate bonded on the top of the gel at time zero. As the solvent molecules can diffuse out of the gel through the permeable plate, the gel thins down progressively.

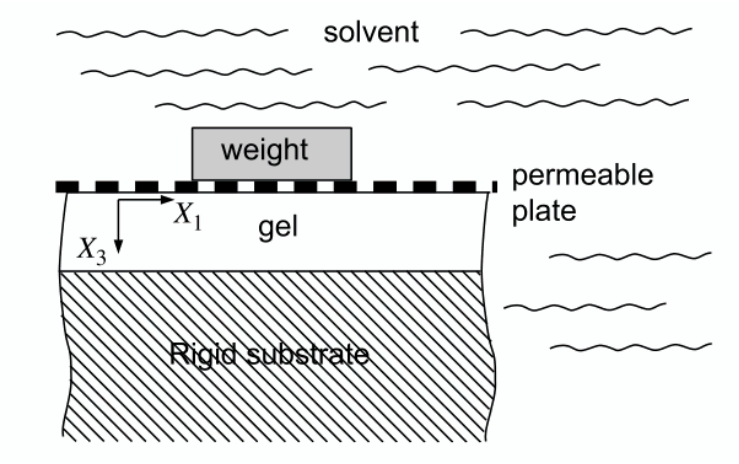

Figure 10. Uniaxial creep problem

Let s be the applied force divided by the area of the dry polymer, X_1, $X_2$and X_3 be the material coordinates in the reference coordinate (the dry and undeformed polymer): X_1 and X_2 in the plane of the layer and X_3 normal to the layer pointing downward as sketched on Figure 10. As previously, the chemical potential of the external solvent is zero. The vapour pressure p_0 is neglected because it is much smaller than s.

2. Initial and final states

The initial state is the swollen gel with $\lambda_1 = \lambda_2 = \lambda_3 = 3.215$. When the solvent migrates out, the vertical stretch λ_3 becomes inhomogeneous and changes with time but the lateral stretches λ_1, λ_2 remain at 3.215 because of the rigid substrate and the thin layer shape. The thickness of the gel is assumed much smaller than the lateral dimensions. Therefore in gel the field is independent of X_1 and X_2 and only the vertical stretch $\lambda_3(X_3, t)$ defined below is determined:

$$\lambda_3(X_3, t) = \frac{\partial x_3(X_3, t)}{\partial X_3} \qquad \textbf{(74)}$$

When the weight is applied on the top of the plane at time 0, the solvent molecules do not first have time to diffuse and the gel has the behaviour of an incompressible elastic body. As the lateral stretches $\lambda_1 = \lambda_2$ are constant, the vertical stretch remains unchanged: $\lambda_3(X_3, 0^+) = 3.215$. After a long time, $t \to \infty$ some small molecules have diffused and the gel reaches a new equilibrium with the weight and the external solvent.

To determine the equation ruling $\lambda_3(X_3, t)$, s_3 is fixed equal to s in equation 44 and μ to 0 in equation 47. This gives two expressions for the osmotic pressure Π:

$$\Pi = \frac{1}{\lambda_1^2}[NkT(\lambda_3 - \lambda_3^{-1}) - s] = -\frac{kT}{\upsilon}\left[log\left(\frac{\upsilon C}{1+\upsilon C}\right) + \frac{1}{1+\upsilon C} + \frac{\chi}{(1+\upsilon C)^2}\right] \qquad \textbf{(75)}$$

The condition of molecular incompressibility is given by:

$$det(F) = 1 + \upsilon C = \lambda_1\lambda_2\lambda_3 = \lambda_1^2\,\lambda_3 \qquad \textbf{(76)}$$

This expression is inserted in equation 75. The rearrangement of this equation gives the expression of $\lambda_3(X_3, t)$ as a function of s:

$$\frac{s\upsilon}{kT} = N\nu(\lambda_3 - \lambda_3^{-1}) + \lambda_1^2 log\left(1 - \frac{1}{\lambda_3\lambda_1^2}\right) + \frac{1}{\lambda_3} + \frac{\chi}{\lambda_3^2\lambda_1^2} \quad \textbf{(77)}$$

The resolution of equation 77 gives $\lambda_3(X_3, \infty)$ for any given value of s.

3. Vertical stretch evolution between 0^+ and ∞

When t increases, the vertical stretch $\lambda_3(X_3, t)$ evolves from $\lambda_3(X_3, 0^+) = 3.215$ to $\lambda_3(X_3, \infty)$ and the evolution spreads from the top surface toward the inside of the gel. The change process is controlled by a Partial Differential Equation (PDE) for the function $\lambda_3(X_3, t)$. This PDE can be derived from the model of Hong et al. First, as $\det(F) = \lambda_1^2\,\lambda_3, F_{33} = \lambda_3$ and $H_{33} = \lambda_3^{-1}$, the equation 36 becomes:

$$s_3(X_3, t) = \frac{\partial W_s}{\partial \lambda_3} - \lambda_1^2 \Pi(X_3, t) \quad \textbf{(78)}$$

The mechanical equilibrium given by equations 13 and 14 is established when the stress $s_3(X_3, t)$is homogeneous and equal to s throughout the gel. On the other hand, the chemical potential μ is inhomogeneous and changes with time like $\lambda_3(X_3, t)$. Recalling equation 37, μ is given by:

$$\mu(X_3, t) = \frac{dW_m}{dC} + \nu\Pi(X_3, t) \quad \textbf{(79)}$$

Using equation 76 and $H_{33} = \lambda_3^{-1}$, the diffusion coefficient of equation 56 becomes:

$$M_{33} = \frac{D}{\nu kT\lambda_3^2}(\lambda_1^2\lambda_3 - 1) \quad \textbf{(80)}$$

Therefore, the kinetic law 48 becomes:

$$J(X_3, t) = -M_{33}\frac{\partial \mu}{\partial X_3} = -\frac{D(\lambda_1^2\lambda_3 - 1)}{\nu kT\lambda_3^2}\frac{\partial \mu(X_3, t)}{\partial X_3} \quad \textbf{(81)}$$

As no solvent molecules are injected in this problem, the equation of conservation 18 becomes:

$$\frac{\partial C(X_3, t)}{\partial t} = -\frac{\partial J(X_3, t)}{\partial X_3} \quad \textbf{(82)}$$

The condition of molecular incompressibility 76 gives a relation between the evolution of the concentration C and $\lambda_3(X_3, t)$:

$$\frac{\partial C(X_3, t)}{\partial t} = \frac{\partial}{\partial t}\left(\frac{\lambda_1^2\lambda_3 - 1}{\nu}\right) = \frac{\lambda_1^2}{\nu}\frac{\partial \lambda_3}{\partial t} \quad \textbf{(83)}$$

Using equations 81 and 82, the variation of $\lambda_3(X_3, t)$ becomes:

$$\frac{\partial \lambda_3}{\partial t} = D\frac{\partial}{\partial X_3}\left[\left(1 - \frac{1}{\lambda_1^2\lambda_3}\right)\frac{1}{\lambda_3}\frac{\partial}{\partial X_3}\left(\frac{\mu(X_3, t)}{kT}\right)\right] \quad \textbf{(84)}$$

With μ=0, the condition of incompressibility 76 and the expression 75 for Π, equation 47 gives:

$$\frac{\mu(X_3, t)}{kT} = log\left(1 - \frac{1}{\lambda_1^2\lambda_3}\right) + \frac{1}{\lambda_1^2\lambda_3} + \frac{\chi}{\lambda_1^4\lambda_3^2} + \frac{N\nu}{\lambda_1^2}\left(\lambda_3 - \frac{1}{\lambda_3}\right) \quad \textbf{(85)}$$

Deriving this expression and inserting it in equation 84 provides the PDE for the function $\lambda_3(X_3, t)$:

$$\frac{\partial \lambda_3}{\partial t} = D\frac{\partial}{\partial X_3}\left[\left(1-\frac{1}{\lambda_1^2\lambda_3}\right)\left(\frac{1}{(\lambda_1^2\lambda_3-1)\lambda_1^2\lambda_3^3}-\frac{2\chi}{\lambda_3^4\lambda_1^4}+\frac{N\upsilon}{\lambda_1^2\lambda_3}\left(1+\frac{1}{\lambda_3^2}\right)\right)\frac{\partial \lambda_3}{\partial X_3}\right] \quad \textbf{(86)}$$

4. Boundary conditions and initial condition

To solve the PDE for $\lambda_3(X_3,t)$, boundary conditions should be determined at $X_3=0$ and $X_3=L$.

a) Boundary condition at X_3=0

On the surface of the gel at $X_3=0$, the small molecules exchange much faster between the external solvent and the gel than they diffuse into the gel inside. Therefore there is always local chemical equilibrium at $X_3=0$, *i.e.* $\mu(0,t)=0$. Using the same process as for equation 69, $\lambda_3(0,t)$ can be determined with the following equation knowing $\lambda_1 = 3.215$ and s:

$$\lambda_1^2\left[log\left(1-\frac{1}{\lambda_3\lambda_1^2}\right)+\frac{1}{\lambda_3\lambda_1^2}+\frac{\chi}{\lambda_3^2\lambda_1^4}+\frac{N\upsilon}{\lambda_1^2}\left(\lambda_3-\frac{1}{\lambda_3}\right)\right]_{X_3=0}-\frac{s\upsilon}{kT}=0 \quad \textbf{(87)}$$

b) Boundary condition at X_3=L

At $X_3=L$, the flux $J(L,t)$ is zero since the rigid substrate is impermable to the solvent. J is function of the concentration gradient $\partial C/\partial X_3$ and the concentration C is a linear function of $\lambda_3(X_3,t)$ because of the molecular incompressibility. Consequently, the flux is proportional to the vertical stretch gradient $\partial\lambda_3/\partial X_3$ and the boundary condition at $X_3=L$ is:

$$\frac{\partial \lambda_3(L,t)}{\partial X_3}=0 \quad \textbf{(88)}$$

c) Initial condition

As the initial state is the swollen gel, the initial condition is $\lambda_3(X_3,0)=3.215$.

5. Resolution of the PDE for the function $\lambda_3(X_3,t)$

The partial differential equation for the vertical stretch $\lambda_3(X_3,t)$ can now be solved. The coefficients are fixed using the constants defined previously: $N\upsilon=10^{-3}, \chi=0.2, D=8\times 10^{-10}$ and $\lambda_1=3.215$.

a) Evolution of the vertical stretch with time

The nominal stress $s\upsilon/kT$ is set at -0.05. The root of the function 87 is found using the Matlab function fzero: the vertical stretch on the top is $\lambda_3(0,t)=0.8183$. The Matlab program is in the appendix.

The PDE is solved numerically using the function pdepe of Matlab which can solve initial-boundary value problems for parabolic-elliptic PDEs in one space variable x and time t. Here x is the dimensionless variable X_3/L.

To use pdepe, the system of partial differential equation must be of the form:

$$c(x,t,u,Du/Dx) * Du/Dt = x\text{^}(-m) * D(x\text{^}m * f(x,t,u,Du/Dx))/Dx + s(x,t,u,Du/Dx) \quad \textbf{(89)}$$

Therefore, u is the function $\lambda_3(X_3,t)$. m and s are set at 0, c at 1. The function f is:

$$f\left(x,t,u,\frac{Du}{Dx}\right)=D\left(1-\frac{1}{\lambda_1^2u}\right)\left[\frac{1}{(\lambda_1^2u-1)\lambda_1^2u^3}-\frac{2\chi}{u^4\lambda_1^4}+\frac{N\upsilon}{\lambda_1^2u}\left(1+\frac{1}{u^2}\right)\right]\frac{Du}{Dx} \quad \textbf{(90)}$$

The boundary conditions at x=a and x=b for all t must be of the form:

$$p(x,t,u) + q(x,t) * f(x,t,u,Du/Dx) = 0 \qquad \textbf{(91)}$$

Consequently, at x=a=0, p(x,t,u)=u-0.8183 and q=0. At x=b=1, p=0 and q=(Du/Dx)/f.

The full Matlab program can be found in the appendix. It provides the evolution of $\lambda_3(X_3,t)$ as a function of the dimensionless coordinate X_3/L for several times as shown on following chart.

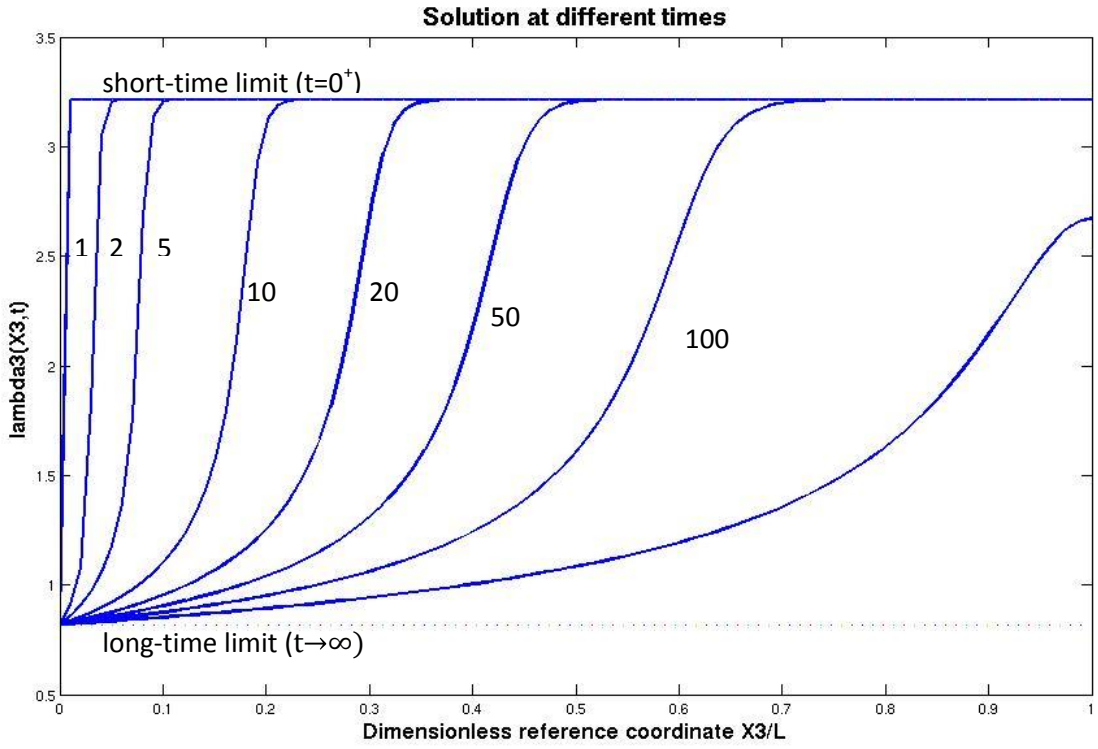

Figure 11. Vertical stretches in the thickness of the gel subject to a nominal stress vs/kT =-0.05 for different times

Consequently, this Matlab program provides the same result as Hong et al (2008a). First, the vertical stretch $\lambda_3(X_3,t)$ changes only on the top surface and remains unchanged inside the gel. When t increases, the stretch inside the gel changes from the short-time limit to the long-time limit the modification propagates progressively from the top surface toward the depth of the gel.

b) Evolution of the thickness according to the stress s

The thickness of the gel is assessed as a function of time for different weights. The vertical stretch on the top surface $\lambda_3(0,t)$ is found as previously for each value of $s\upsilon/kT$ and given in the table below.

$s\upsilon/kT$	-0.03	-0.05	-0.1	-0.2
$\lambda_3(0,t)$	1.0358	0.8183	0.5949	0.4358

Table 2. Values of $\lambda_3(0,t)$ according to the weight

The PDE for the function $\lambda_3(X_3,t)$ is solved as previously. Then the vertical strecth is integrated to obtain the thickness of the gel. The Matlab program provides the following chart of the dimensionless thickness l/L as a function of $\sqrt{tD/L^2}$.

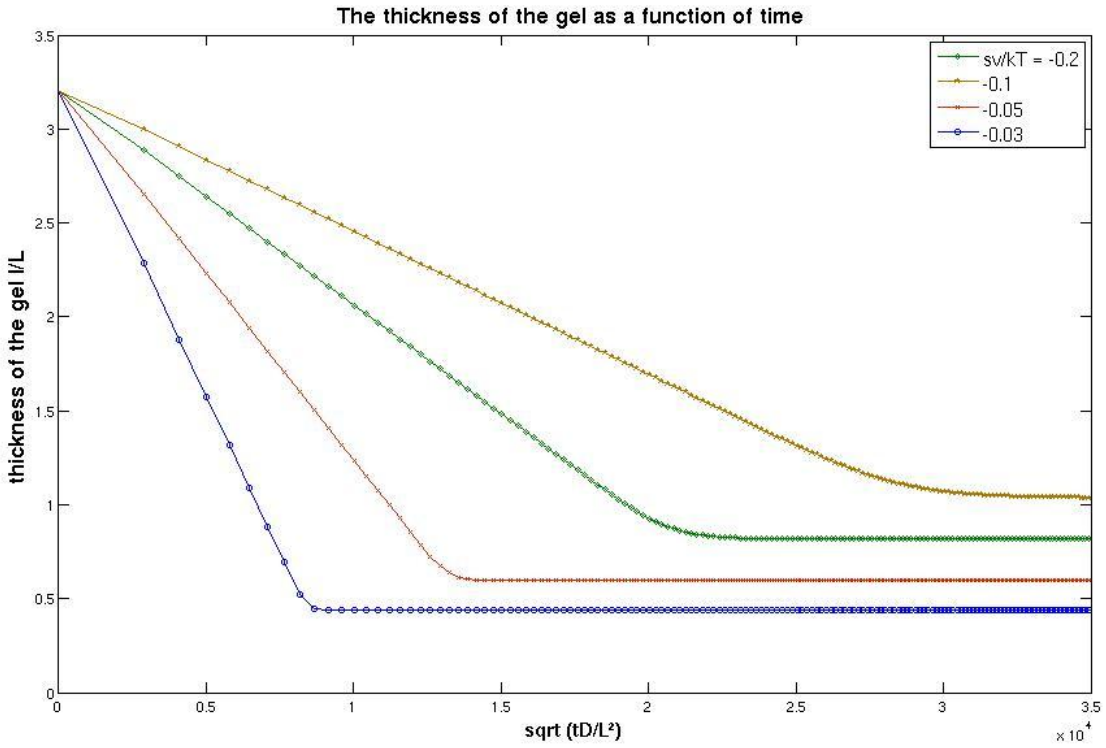

Figure 12. Thickness of the gel as a function of time for different values of weights

This chart is the same as the result of Hong et al. (2008a). At time $t = 0^+$, the dimensionless thickness of the gel is equal to that of free swelling: $\mathrm{l/L} = 3.215$. Then, there are two stages in the diffusion process. Initially, when $t \ll L^2/D$, the solvent molecules diffuse only near the top surface, so the diffusion rate does not depend on the thickness of the gel L. Therefore, no length scale exists in the problem and the vertical stretch $\lambda_3(X_3,t)$ follows the self-similar profile described in the next paragraph. In this part, the decrease of the thickness is linear in $\sqrt{Dt}$. In the second stage corresponding to $t \gg L^2/D$, the thickness becomes constant reaching the longtime limit.

c) Self-similar solution

The self-similar solution is examined for an infinitely thick layer. No length scale exists in the problem in the initial value problem. Therefore, the vertical stretch $\lambda_3(X_3,t)$ must take the form:

$$\lambda_3(X_3,t) = \lambda_3(\xi) \quad with\ \xi = X_3/\sqrt{Dt} \tag{92}$$

The definition of ξ gives the following identities for the derivatives:

$$\frac{\partial}{\partial X_3} = \frac{\partial \xi}{\partial X_3}\frac{\partial}{\partial \xi} = \frac{1}{\sqrt{Dt}}\frac{\partial}{\partial \xi} \tag{93}$$

$$\frac{\partial}{\partial t} = \frac{\partial \xi}{\partial t}\frac{\partial}{\partial \xi} = -\frac{X_3}{2t\sqrt{Dt}}\frac{\partial}{\partial \xi} = \frac{\xi}{2t}\frac{\partial}{\partial \xi} \tag{94}$$

Therefore, equation 86 becomes the following ordinary differential equation (ODE):

$$\left(1-\frac{1}{\lambda_1^2\lambda_3}\right)\left[\frac{1}{(\lambda_1^2\lambda_3-1)\lambda_1^2\lambda_3^3}-\frac{2\chi}{\lambda_3^4\lambda_1^4}+\frac{N\nu}{\lambda_1^2\lambda_3}\left(1+\frac{1}{\lambda_3^2}\right)\right]\frac{d^2\lambda_3}{d\xi^2}+\frac{\xi}{2}\frac{d\lambda_3}{d\xi}$$
$$+\left[-\frac{4}{\lambda_1^4\lambda_3^5}+2\chi\frac{4\lambda_1^2\lambda_3-5}{\lambda_1^6\lambda_3^6}+\frac{N\nu}{\lambda_1^4\lambda_3^5}(4-3\lambda_1^2\lambda_3+2\lambda_3^2-\lambda_1^2\lambda_3^3)\right]\left(\frac{d\lambda_3}{d\xi}\right)^2=0 \quad \textbf{(95)}$$

This ODE is transformed into a system of first order ODE:

$$y_2=\frac{d\lambda_3}{d\xi} \quad \textbf{(96)}$$

$$\frac{d}{d\xi}[f(y_I)y_2]+\frac{\xi}{2}y_2=0 \;\; where\; y_I=\lambda_3 \quad \textbf{(97)}$$

$$and\;\; f(\lambda_3)=\left(1-\frac{1}{\lambda_1^2\lambda_3}\right)\left[\frac{1}{(\lambda_1^2\lambda_3-1)\lambda_1^2\lambda_3^3}-\frac{2\chi}{\lambda_3^4\lambda_1^4}+\frac{N\nu}{\lambda_1^2\lambda_3}\left(1+\frac{1}{\lambda_3^2}\right)\right] \quad \textbf{(98)}$$

This system of ordinary differential equations is integrated numerically on the interval [a, b]= [0,$L/\sqrt{Dt}$] using the function bvp4c of Matlab. The two-point boundary value conditions is defined by $y_I=\lambda_3(0,t)$ at $\xi=0$ and $y_2=0$ at $\xi=L/\sqrt{Dt}$. The initial value is given by $y_I=3.215$. The full Matlab program can be found in the appendix. The plot provided by this program is presented in Figure 13. The function $\lambda_3(\xi)$ is plotted for different levels of the applied weight, which gives the same results as Hong et al. (2008a). Two regions separated by a diffusion front can be distinguished in the layer. At the rear of the front, the gel is close to the long-time limit $\lambda_3(0)$. Ahead of the front, the gel is near the short-time limit $\lambda_3(\xi)=3.215$.

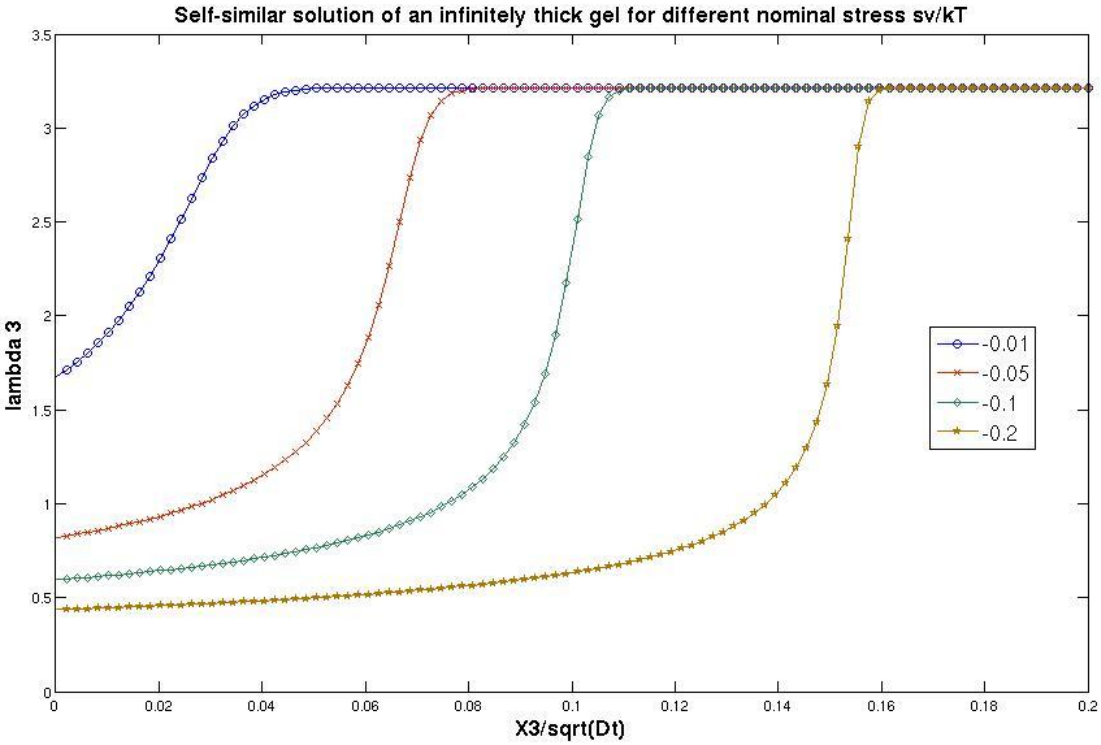

Figure 13. Self-similar solution of an infinitely thick gel

Chapter 3 : Numerical implementation

The model described in the second chapter has been implemented using Comsol Multiphysics, finite element software. The general equations summarised previously are implemented and the two problems previously solved analytically are resolved with Comsol Multiphysics. The main characteristics of the software utilized are presented. Then the steps of the implementation are explained.

I. Generalities about the software

COMSOL Multiphysics (formerly FEMLAB) is software which allows the analysis and resolution of problem by the finite element method. It enables to solve various physics and engineering problems, in particularly multiphysics or coupled phenomena such as thermal and mechanics.

COMSOL Multiphysics permits the resolution of general Partial Differential Equations (PDEs) and Variational Form. It contains several predefined modules such as the chemical engineering and structural mechanics modules. Therefore some common PDEs can be used directly by simply defining the corresponding coefficients. However the user can also define his own PDE or Weak Form or redefine some variables such as the free energy function. As COMSOL Multiphysics has an interface with MATLAB, the user can define constants or functions using the MATLAB programming syntax. A similar interface exists in COMSOL Script which enables to write program for COMSOL Multiphysics or to modify the program generated using the graphical user interface.

Initially the model was implemented in COMSOL 3.4 before switching to the COMSOL 3.5. This version is interesting because a segregated solver is available for time-dependent problems and not limited anymore to stationary ones. This solver enables memory usage cut for solving classical multiphysics.

II. Implementation

A. Predefined modules

Two predefined modules were used: structural mechanics and diffusion. Both were transient analysis. The structural mechanics models were the solid stress-strain in three dimensions or the plane strain in two dimensions.

B. Constants and functions

The constants and functions of the model are defined in the options. The constants are the constant identified in the previous chapter and some defining the boundary conditions such as concentration, chemical potential, pressure and displacement. The functions defined as scalar expressions with Matlab syntax are the chemical potential, the elements of the diffusion coefficient matrix, the free energy function. The tables of the constants and functions can be found in the appendix.

C. Geometry

A cube is drawn to define the problem of free swelling. The first corner of the cube is at the coordinate (0, 0, 0) and the cube side length L is chosen at 0.1m. The creep uniaxial test can be either implemented with this cube or a thin layer (of thickness L/10 for example).

D. Structural mechanics

- **Subdomain settings:** The material of the cube is chosen hyperelastic. The mixed U-P formulation is used to define the material as nearly incompressible.
- **Boundary settings:** Three faces are blocked to avoid rigid body motion. A pressure is imposed on the top face in the implementation of the creep uniaxial problem.
- **Properties:** Large deformation option is selected.
- **Model settings:** The equation system is chosen as weak form (for the multiphysics problem).
- **Equation system- Subdomain settings:**
    - A new free energy function is defined as Ws_smsld_2 in the scalar expressions. This function is used in the definition of the Pioley-Kirshoff tensor: Px= diff(Ws_smsld_2,ux)
    - The condition of incompressibility is modified to add the term υC: p_test*(-1+p/kappa_smsld+Jel_smsld-vol*c)

E. Diffusion

- **Subdomain settings:** The classical PDE of diffusion is predefined. The coefficient of diffusion is defined by the function dij defined previously in the scalar expression.
- **Boundary settings:** The concentration or the flux can be imposed at the top boundary.
- **Model settings:** The equation system is chosen as weak form.

F. Mesh

The mesh is created using the free mesh parameters. The mesh is initially chosen extra coarse and then refined everywhere or in some areas with the boundary or edge mesh parameters.

G. Solver

- **Solver parameters:**
    - *Time-dependent solver:*

Firstly a time dependent solver is used with COMSOL Multiphysics 3.4. Then the time-dependent segregated solver is used with the version 3.5: it allows splitting the solution steps into substeps solving either mechanical or diffusion problem. Moreover this solver enables to choose different linear system solvers for each kind of substep (mechanical or diffusion here).

- *Direct/ iterative solver*:

A direct solver can be used for 2D models and for 3D models with few degrees of freedom (approximatively 100,000 to 1,000,000 depending on available memory).These solvers solve the linear system by Gaussian elimination. This process is stable and reliable and well suited even for ill-conditioned system. However the elimination mechanism can require large memory resources and long computation times, which is a problem for 3D models. In Comsol, the direct linear solvers that can be used to solve symmetric and non symmetric systems are UMFPACK, SPOOLES and PARDISO. PARDISO is a highly efficient direct solver for symmetric and nonsymmetric systems. UMFPACK is

also highly efficient for nonsymmetric systems but uses more memory than PARDISO. SPOOLES is less efficient than UMFPACK but uses also less memory.

Since the direct solvers require usually too much memory for models with many degrees of freedom, an iterative solver which is more memory-efficient will perform better. Nevertheless, iterative solvers are less stable than directs ones and do not always converge. The convergence of iterative solvers can be improved by using an appropriate preconditioner. In Comsol, the iterative solvers that can be used to solve symmetric and non symmetric systems are GMRES and FGMRES which handle more general preconditioners but uses more memory than GMRES. These two iterative solvers can be used with the Incomplete LU preconditioner.

- *Time stepping*:

The intervals of resolution and time steps are fixed. For example a time stepping 0:1:5 corresponds to the resolution of the PDEs on an interval [0, 5] with time steps of 1.

- **Solver manager:** The model is solved for both mechanical and diffusion physics. The solution of the free swelling problem can be stored and used as initial values for the creep uniaxial problem.

III. Basic validations

The implementation of the model of Hong et al (2008a) is carried out step by step. First the mechanical and diffusion model are implemented separately in 2D plain strain models and 3D strain-stress models.

A. Mechanics

Some compression tests are performed on a cube of hyperelastic material: the bottom is fixed and a pressure p is applied on the top as sketched on Figure 14.

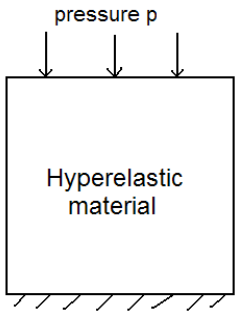

Figure 14. Compression test on a hyperelastic cube

First, the hyperelasticity is modelled with Neo-Hookean model. If the imposed pressure is set constant at p1=5e2 Pa, Comsol Multiphysics cannot find the solution: the direct linear solver does not converge. Secondly, the pressure is applied progressively by using the following function:

p2= [p1*0.5*(1+tanh(2[s^-1]*(t-2.5[s])))] **(99)**

Comsol can now compute the solution of this simple problem. Therefore the brutal changes in the boundary load should be avoided.

The free energy function Ws_smpn is now redefined with the Flory-Huggins model: Ws_smpn_2=0.5*NkT*(-3+I1_smpn-log(I3_smpn)). As explained before, the Pioley-Kirshoff tensor is redefined with this new free energy function. The same compression test is carried out with a pressure constant p and with the pressure function p2. The first test works on 0:0.5:100 but the computation is very slow. The second test works properly. Consequently, the brutal changes in the applied pressure should again be avoided.

Then this compression test case is implemented in 3D with the same procedure. It works properly if the pressure is imposed gradually like the 2D model.

B. Diffusion with problem of boundary conditions

Some simple diffusion tests are carried out on a square insulated on three sides as sketched on Figure 15. Different boundary conditions are imposed on the top: fixed concentration, flux or chemical potential. The initial concentration is zero corresponding to a dry polymer.

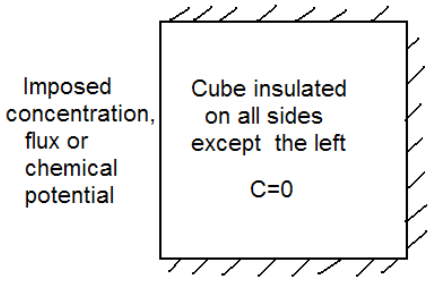

Figure 15. 2D diffusion test

The diffusion PDE for the concentration is predefined as equation 63 (b). The implemented diffusion coefficient is the chemical part of D_{KL} given previously in equation 69:

$$Dij=(D1/(1+vol*c)^2)*(1-2*ksi*vol*c/(1+vol*c)) \quad \textbf{(100)}$$

1. 2D diffusion model

a) Imposed concentration

In the model presented in chapter 2, the chemical boundary condition is either a fixed flux or chemical potential. Nevertheless, imposing a concentration on a boundary can enable to reach a state of uniform concentration such as a swollen gel in chemical equilibrium.

In the first test, a constant concentration Ce1=$5e4\ mol/m^3$ is imposed on the left. The resolution on 0:0.5:100 works: the final state of homogeneous concentration is reached. Then the imposed concentration is increased to Ce1=$8e4\ mol/m^3$. In that case, Comsol Multiphysics cannot find the final solution: it cannot find consistent initial condition and the direct linear solver does not converge. Subsequently, the boundary concentration is increased progressively from 0 to Ce1 with the following function:

$$Ce2= [Ce1*0.5*(1+tanh(2[s^-1]*(t-2.5[s])))] \quad \textbf{(101)}$$

The solver converges and the final state of uniform concentration is reached. Therefore the variation of concentration on the boundary should not be too fast.

a) Imposed chemical potential

I have tried to impose a zero value for the chemical potential μ on the left boundary by adding a multiphysics weak form on this boundary. The new weak variable is lamb. The chemical potential is imposed using the boundary settings of this new weak form: the weak condition test(lamb)*mu+test(c)*lamb is fixed on the left boundary. The chemical potential μ was defined in the scalar expression by:

Mu = kT*(log(vol*c/(1+vol*c))+1/(1+vol*c)+ksi/(1+vol*c)^2) **(102)**

Unfortunately, COMSOL cannot solve the diffusion problem with this condition. I have tried to impose other expressions for the chemical potential. If Mu = kT*(1- c + ksi*(1-c)^2). Then COMSOL can solve the diffusion problem with a chemical potential on the boundary. If Mu = kT*(log(c+ceps)+ 1- c + ksi*(1-c)^2) with ceps=1e-3, COMSOL cannot solve the problem. In conclusion, it seems that the chemical potential of the model of Hong et al. (2008a) cannot be imposed on a boundary, probably because the log function and μ goes to $-\infty$ when c vanishes.

b) Imposed flux

In the model of Hong et al. (2008a), the flux J is proportional to the gradient of chemical potential μ. The chemical part of J is:

$$J = -\frac{D}{kT\upsilon}\frac{\partial \mu}{\partial X} \quad \textbf{(103)}$$

Therefore a flux proportional to the variation of μ can be imposed on the boundary:

$$J = -\frac{D}{kT\upsilon}\frac{(\mu - \mu_{imp})}{dx} = -atte\left(\mu - \mu_{imp}\right) \quad with\ \mu_{imp} = 0 \quad \textbf{(104)}$$

Since the chemical potential goes to $-\infty$ when c vanishes, a small concentration ceps is added in the log function of μ:

$$\mu = kT\left[log\left(\frac{\upsilon(C + Ceps)}{1 + \upsilon C}\right) + \frac{1}{1 + \upsilon C} + \frac{\chi}{(1 + \upsilon C)^2}\right] \quad \textbf{(105)}$$

ceps and dx are respectively set to $1\mathrm{e}-9\ \mathrm{mol/m^3}$ and $1\mathrm{e}-10\ \mathrm{m}$. This problem is solved with a COMSOL direct solver. After 2.2e9 s, the stationary state is almost reached: J =0.0998 and c=3.318e9 $\mathrm{mol/m^3}$in the middle of the cube. The final state is attained after 9e14s. Figure 16 shows the concentration in the model after 1e10s.

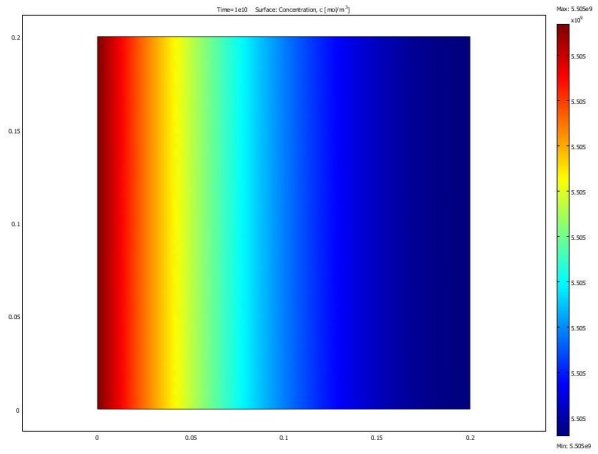

Figure 16. Concentration in the 2D diffusion model at 1e10s

2. 3D diffusion model

a) Imposed concentration

First a constant concentration Ce1=$5\mathrm{e}2\ \mathrm{mol/m^3}$ is imposed on the top boundary. COMSOL can solve this problem on 0:0.5:100 with a direct linear solver. Secondly, the concentration is increased to Ce1=$5.35\mathrm{e}5\ \mathrm{mol/m^3}$ and COMSOL cannot solve the problem anymore. Subsequently, the boundary concentration is increased progressively from 0 to Ce1 with the following function as previously. However even with the very slow function Ce2= Ce1*0.5[1+tanh(0.002(t-2500))] and a very fine mesh represented on , COMSOL cannot solve this problem on 0:2000:120000: the direct solver failed at time 2423. The final concentration is only Cend=$2.293e5 mol/\mathrm{m^3}$. Nevertheless, this final solution is better than the one with coarser meshes: the COMSOL solver fails earlier in these cases.

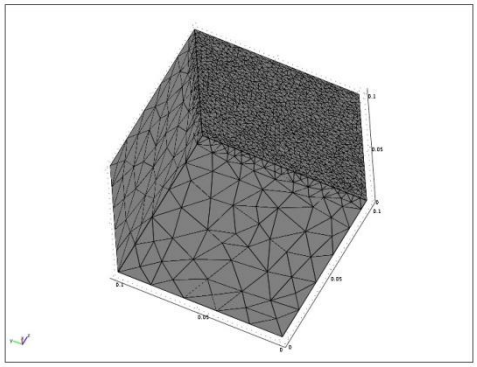

Figure 17. 7595 tetrahedral element mesh used to impose the concentration on one side

A uniform final concentration of Cend=$5.35\mathrm{e}5\ \mathrm{mol/m^3}$ can nonetheless be obtained using the boundary condition: Ce2=Ce1*0.5*(1+tanh(2e-5[s^-1]*(t-2.5e5[s]))) on 0:2e4:1.2e6 with a coarse mesh.

In conclusion, to impose a concentration on one boundary of a 3D cube, the concentration should increase very slowly with time. Moreover, since the diffusion is very slow, the molecules are first

concentrated in the first layer of elements. Therefore, a finer mesh on the boundary with an imposed concentration can help the solver to converge.

3. Imposed chemical potential

Imposing the chemical potential on the left boundary raises the same problem as for the 2D model. Therefore the chemical potential will not be imposed.

4. Imposed flux with different expressions

The flux is imposed in the same way as the 2D case with no more problems.

Chapter 4 : Results

After the previous basic validations, the full coupled model of Hong et al. (2008a) can be implemented in COMSOL Multiphysics. Then the free swelling and creep uniaxial problems are solved in 2D and 3D, the goal being to find the same results as previously.

I. Free swelling of a cube

A. Free swelling of a cube in 2D

First a 2D plain-strain model is used. The geometry is a square of length side L=0.1m with a thickness L. To avoid rigid body motion, the square is bloked as sketched on Figure 18. For the chemical problem, a flux $J = -atte\,(\mu - \mu_{imp})$ is imposed on one side and the other boundaries are insulated. μ_{imp} is zero and atte is set at 1e18. Consequently, the chemical potential μ should be equal to $\mu_{imp} = 0$ on the boundary where the flux is imposed.

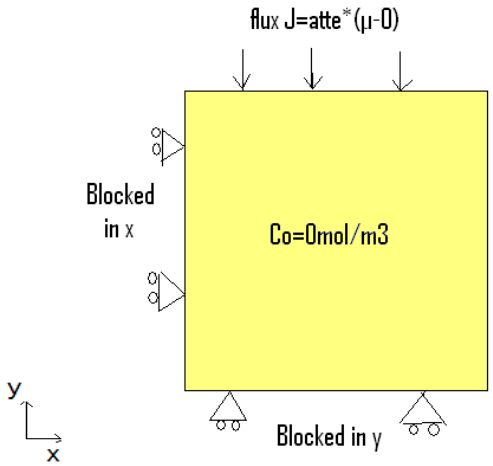

Figure 18. 2D free swelling model

As previously, to avoid problem when C vanishes, a ceps is added to the log function of the chemical potential:

$$\mu = kT\left[log\left(\frac{\upsilon(C+Ceps)}{1+\upsilon C}\right) + \frac{1}{1+\upsilon C} + \frac{\chi}{(1+\upsilon C)^2}\right] + \Pi\upsilon \qquad \textbf{(106)}$$

To obtain μ=0 as a final state, ceps should vanish. Therefore ceps is chosen as a function ceps=ceps1*(1[s]-t*0.1)*(t<10) with $\mathrm{ceps1} = 300\ \mathrm{mol/m^3}$ (as the lowest values raised problems).

The final state should be $\lambda_x = \lambda_y = \lambda_{final}$ and $\lambda_z = 1$. The analytical value of λ_{final} is the root of the following function obtained like equation 77:

$$0 = N\nu\left(\lambda_{final} - \lambda_{final}^{-1}\right) + \lambda_{final}\,log\left(1 - \frac{1}{\lambda_{final}^2}\right) + \frac{1}{\lambda_{final}} + \frac{\chi}{\lambda_{final}^3} \qquad \textbf{(107)}$$

Then, the analytical value of λ_{final} is 5.765 and $\det(F) = 1 * {\lambda^2}_{final} = 33.231$. Using the incompressibility condition, the final concentration should be $\mathrm{C} = 5.3522\ \mathrm{e}\ 5\mathrm{mol/m^3}$. At the

chemical equilibrium, μ is zero everywhere in the gel and the final osmotic pressure can be calculated from the expression 68: $\Pi = 1.1238\text{e}4$ Pa. Finally, the coefficient NkT can be computed with equation 46 where s=0:

$$NkT = \frac{\Pi\lambda_{final} * 1}{\left(\lambda_{final} - \lambda_{final}^{-1}\right)} = 1.1587e4\ N/m^2 \quad \textbf{(108)}$$

The problem is solved with the segragated time-dependent solver (with PARDISO direct solver for each substep) and a normal mesh on 0 : 5e2 : 3e6. The solver failed before the end of this interval. This problem remains when the mesh is refined or the parameters ceps and atte are modified.

Consequently, the problem of convergence comes more probably from the fact that the diffusion is two slow: $\text{D} = 8\text{e} - 10\ \text{m}^2/s$ and D_{ij} decreases up to $7\text{e} - 14\ \text{m}^2/s$ when the model has almost reached the final state. Then I have decided to transform the diffusion PDE into a dimensionless PDE using characteristic dimension of length, concentration and time: L_0=0.1m, $\text{C}_0 = 1\text{e}5\ \text{mol/m}^3$, $\text{t}_0 = \text{L}^2/\text{D} \approx$ 1e7s. The dimensionless variables are $\text{C}' = \text{C}/\text{C}_0$, $\text{t}' = \text{t}/\text{t}_0$, $\text{L}' = \text{L}/\text{L}_0$ The diffusion PDE becomes:

$$\frac{C_0}{t_0}\frac{\partial C'}{\partial t'} + \frac{C_0}{L_0^2}\nabla'(-D\nabla' C') = 0 \quad \textbf{(109)}$$

The numerical application gives:

$$\frac{\partial C'}{\partial t'} + 10^9\nabla'(-D\nabla' C') = 0 \quad \textbf{(110)}$$

Therefore the diffusion problem can be redefined with a new diffusion coefficient D_2=10^9 ∗D and a concentration $\text{C}_2 = 10^5$ ∗D. Then C is replaced by C_2 in all the functions (μ,Ws,incompressibility).

The same solving parameters as previously now enable to solve the free swelling model. The resolution takes 153.4s. The expected results are found: F11=F22=5.765, $\text{C}_2 = 5.352775\ \text{mol/m}^3$ or $\text{C} = 5.352775\text{e}5\ \text{mol/m}^3$ and $\Pi = 1.1238\text{e}4$ Pa. The evolution of different functions with time are drawn with COMSOL Multiphysics (Cf . Figure 19-22). The chemical potential vanishes progressively as the flux. The stretch F11 and the concentration C increase gradually: fast at the beginning and then more and more slowly.

These results should not be the experimental one for the small concentration because of the hypothesis made about the diffusion coefficient in the model of Hong et al. (2008a).

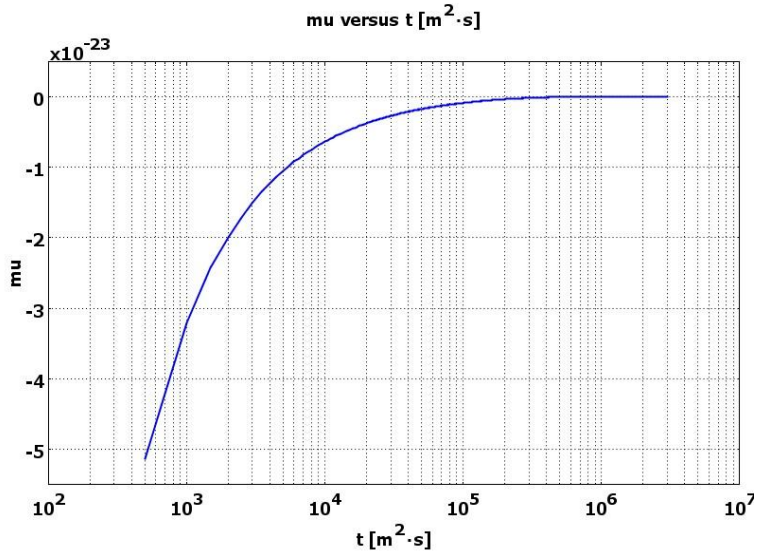

Figure 19. Evolution of the chemical potential with time during swelling

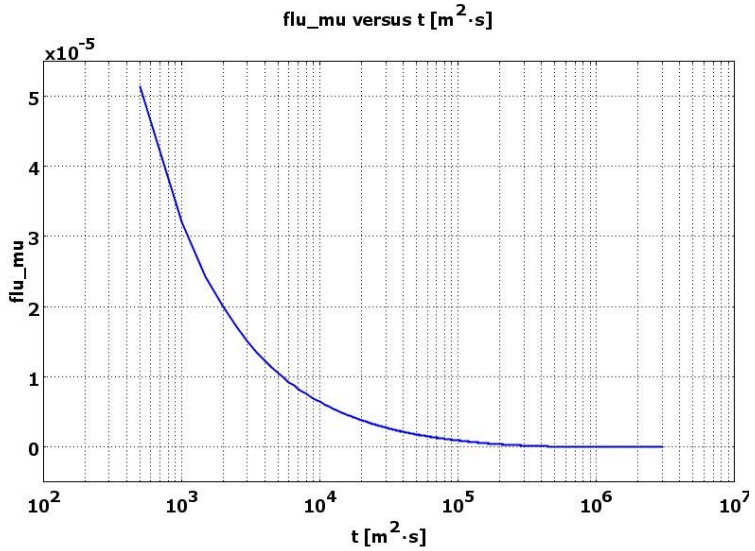

Figure 20. Evolution of the flux with time during swelling

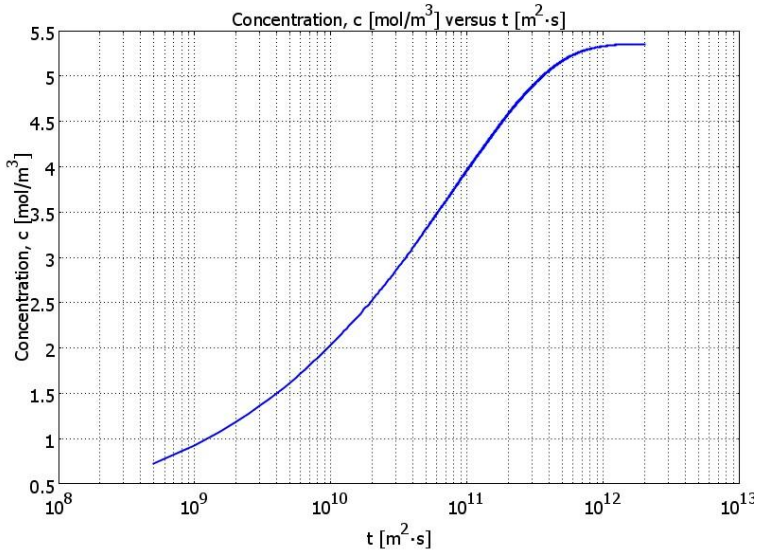

Figure 21. Evolution of the concentration with time during swelling

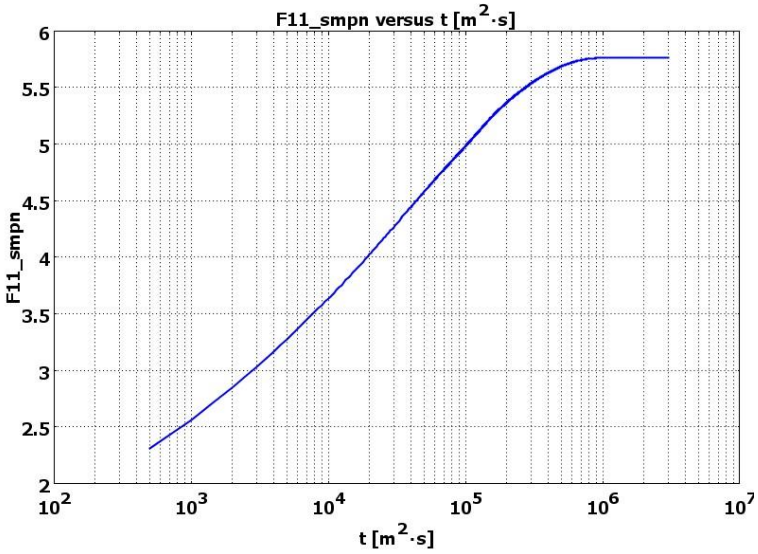

Figure 22. Evolution of the stretch F11 with time during swelling

B. Free swelling of a 3D cube with diffusion on one boundary

A cube of gel is swollen by diffusion throug one boundary as sketched on Figure 23. The geometry is a cube of length side L=0.1m. To avoid rigid body motion, the face 1 (x=0) is bloked in x, the face 2 (y=0) is bloked in y and the face 1 (z=0) is bloked in z. For the chemical problem, a flux $J = -\chi(\mu - \mu_{imp})$ is imposed on the top surface. μ_{imp} is zero and atte is set at 1e10 (the solver will not converge for bigger flux). Consequently, the chemical potential μ should be equal to $\mu_{imp} = 0$ on the boundary where the flux is imposed.

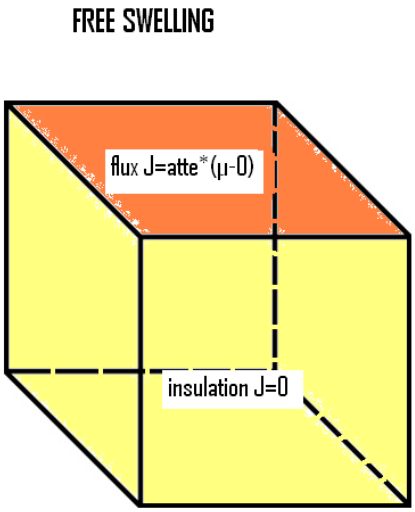

Figure 23. 3D free swelling model

As for the 2D, to avoid problem when C vanishes, a ceps is added to the log function of the chemical potential which gives equation 106. ceps is chosen as a function ceps=ceps1*(1[s]-t*0.1)*(t<10) with $\mathrm{ceps1} = 160\ \mathrm{mol/m^3}$ (as the lowest values raised problems).

As calculated previously, the analytical value of $\lambda_{final} = \lambda_1 = \lambda_2 = \lambda_3$ is 3.215 and $\det(F) = \lambda_{final}^3 = 33.231$. Using the incompressibility condition, the final concentration should be $\mathrm{C} = 5.3522\ \mathrm{e}\ 5\mathrm{mol/m^3}$. At the chemical equilibrium, μ is zero everywhere in the gel and the final osmotic pressure can be calculated from the expression 68: $\Pi = 1.1238\mathrm{e}4\ \mathrm{Pa}$. Finally, the coefficient NkT can be computed with equation 46 where s=0:

$$NkT = \frac{\Pi\lambda_{final}^2}{\left(\lambda_{final} - \lambda_{final}^{-1}\right)} = 4e4\ N/m^2 \qquad \textbf{(111)}$$

Some free swelling tests were carried out with various imposed concentrations and flux. Nevertheless the segragated time-dependent solver (with PARDISO direct solver for each substep) were never able to reach the final swollen state whatever the mesh and the parameters ceps and atte. Therefore, the dimensionless PDE presented before will be also used for the 3D swelling.

This PDE is solved on 0 : 5e10 : 5e14, which takes 42mn. The expected results are found: F11=F22=F33=3.215, $\mathrm{C_2} = 5.352775\ \mathrm{mol/m^3}$ or $\mathrm{C} = 5.352775\mathrm{e}5\ \mathrm{mol/m^3}$ and $\Pi = 1.1238\mathrm{e}4\ \mathrm{Pa}$. The evolution of different functions with time can be drawn with COMSOL Multiphysics. The resulting plots are similar to the ones in 2D.

C. Free swelling of a 3D cube with diffusion on all boundary

Following Zhang (2008), I have tried to swell the cube of polymer on all boundary imposing concentration or flux. The cube is fixed at the center point and the center points of the face (x=0) and (y=0) can translate only in the x and y-directions repectively. As shown on Figure 24, the same results as Zhang (2008) are observed: the corners swell first because they have the largest surface contact with the solvent; the swelling of the corners is followed by the swelling of the edge and then the other part of the gel.

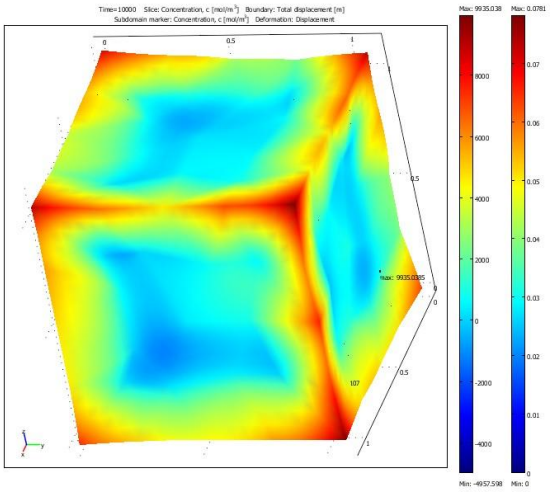

Figure 24. Intermediate free swelling of a cube of polymer immersed in a solvent

II. Creep uniaxial in 2D

Starting from the swollen state, a pressure s is imposed on the cube to achieve the creep uniaxial case explained in the chapter 2. The initial swollen state of this test case can either be done by starting from the stored free swelling or by imposing the concentration and displacements resulting from the free swelling. The imposed pressure s is set to -2e6 Pa which corresponds to sv/kT =-0.05 imposed in the problem solved analytically in chapter 2. The creep case studied in the second chapter was done on a layer of gel. Blocking and insulating the two lateral sides after swelling is equivalent to study the center part of this layer. This displacement of the right boundary can be found in the stored free swelling data: Rx= 0.47646365868934 m. The resulting model is sketched on Figure 25: all displacements are translation on y and the bottom and lateral sides are insulated such that the solvent can only diffuse through the top boundary.

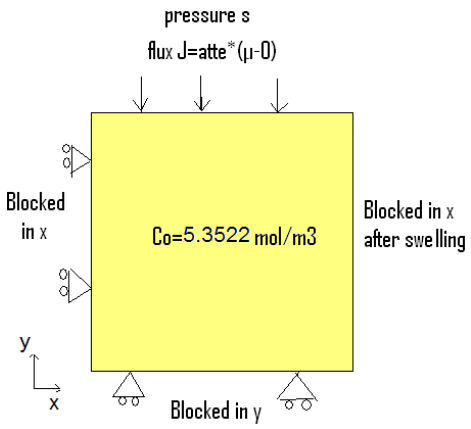

Figure 25. 2D creep uniaxial case

First the dimensionless PDE and the numerical implementation are unchanged compared to the free swelling except for the boundary conditions. Moreover the concentration c will not vanish anymore, ceps is set to 0. The problem is solved with the segragated time-dependent solver (with PARDISO direct solver for each substep) on the time stepping 0:5e1:3e6. At time 3e6, the resolution gives

F11=5.765 and F22=1.115, $C_2 = 0.901\ \mathrm{mol/m^3}$ or $C = 0.901e5\ \mathrm{mol/m^3}$ and $\Pi = 3.474e5$ Pa. This corresponds to the long-time limit value of λ_y computed analytically as the root of the following function with $\lambda_x = 5.765$ unchanged in the creep uniaxial case:

$$N\nu\left(\lambda_y - \lambda_y^{-1}\right) + 1 * \lambda_x log\left(1 - \frac{1}{\lambda_y \lambda_x * 1}\right) + \frac{1}{\lambda_y} + \frac{\chi}{\lambda_y^2 \lambda_x * 1} - \frac{sv}{kT} = 0 \qquad \textbf{(112)}$$

The evolution of F22 and μ with time in the thickness of the gel are plotted and shown on Figure 26 and Figure 27. Therefore, F22 and μ are uniform in the thickness of the gel at any time. They evolve gradually from their short-time limit value to their long-time limit value.

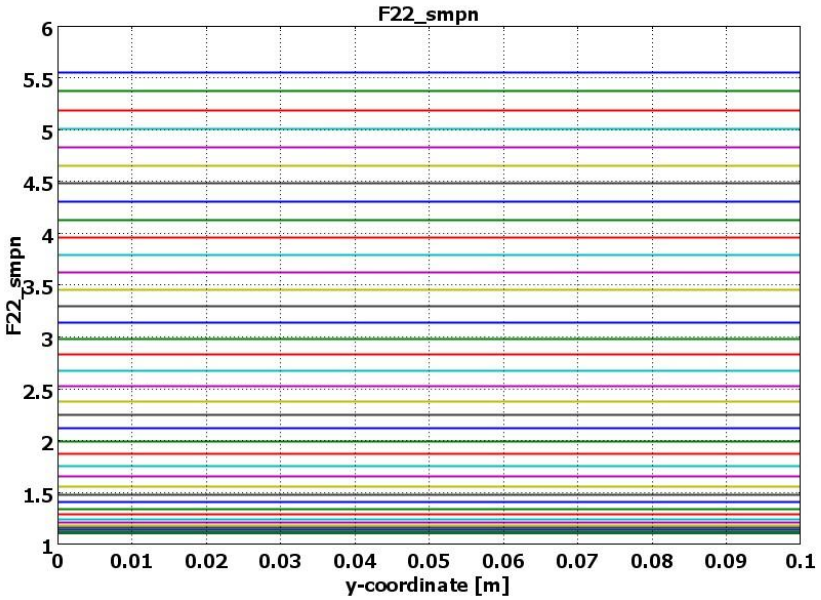

Figure 26. Evolution of F22 with time in the tickness of the gel with D2=8e-1m²/s

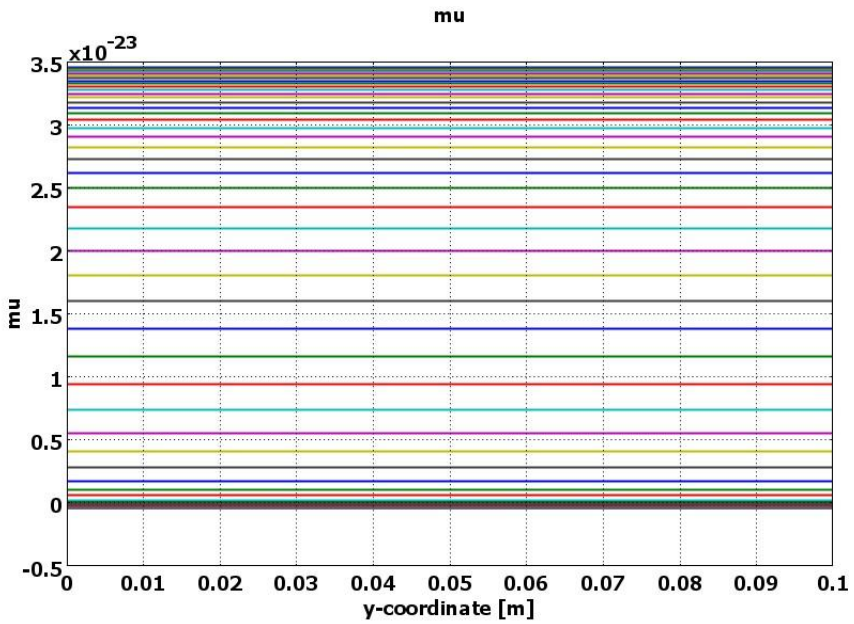

Figure 27. Evolution of μ with time in the tickness of the gel with D2=8e-1m²/s

Consequently, it seems that the diffusion is too fast compared to the mechnical equilibrium: the stretch F22 and the chemical potential are “instantaneously” diffused in the layer of the gel. This can come from the approximation of the flux which could be bigger than approximated when the gradient of μ is almost infinite. However if the coefficient atte is increased, the solver has trouble to converge. Then I have tried to decrease the diffusion coefficient D_2.

After several trials, D_2 is set at 8e-8 m²/s, ceps1 at 2500 and the function ceps is chosen as ceps1*(1[s]-t*0.1)*(t<10). The problem is solved on 0:5e3: 12e6. The results are very close to the analytical solution with y pointing upward instead of downward previously ($y=-X_3$): F22 has the same variations as λ_3 between the short-time and long-time limit values (different from the 3D ones) in the thickness of the gel. The evolution of the thickness is also similar. The self-similar solution is a bit different from the analytical solution. The chemical potential variation is close to the solution found by Zhang et al (2008).

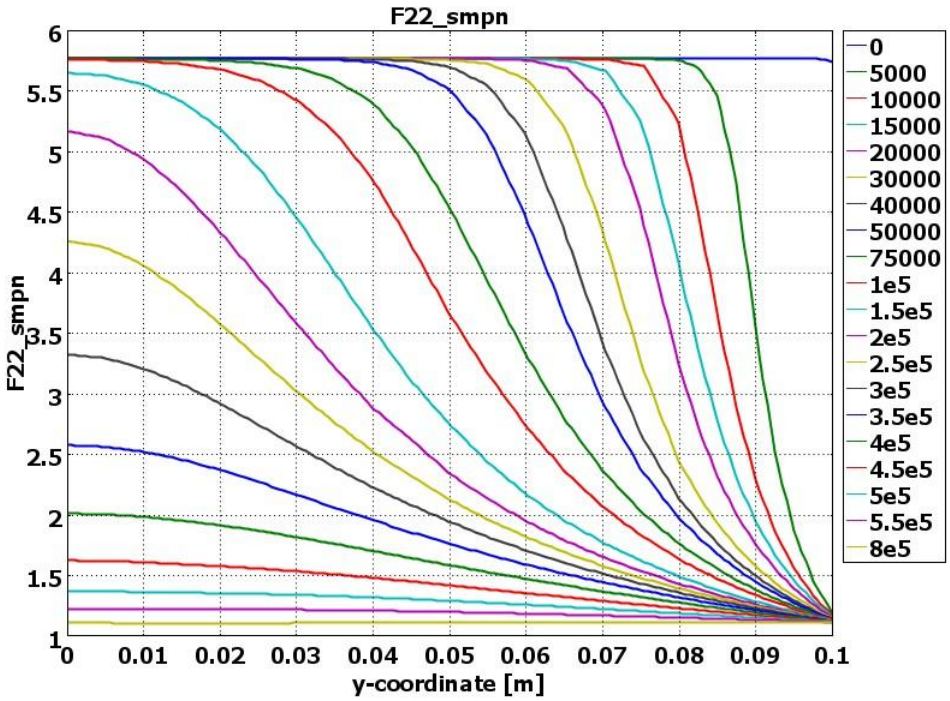

Figure 28. Evolution of the vertical stretch in the thickness of the gel

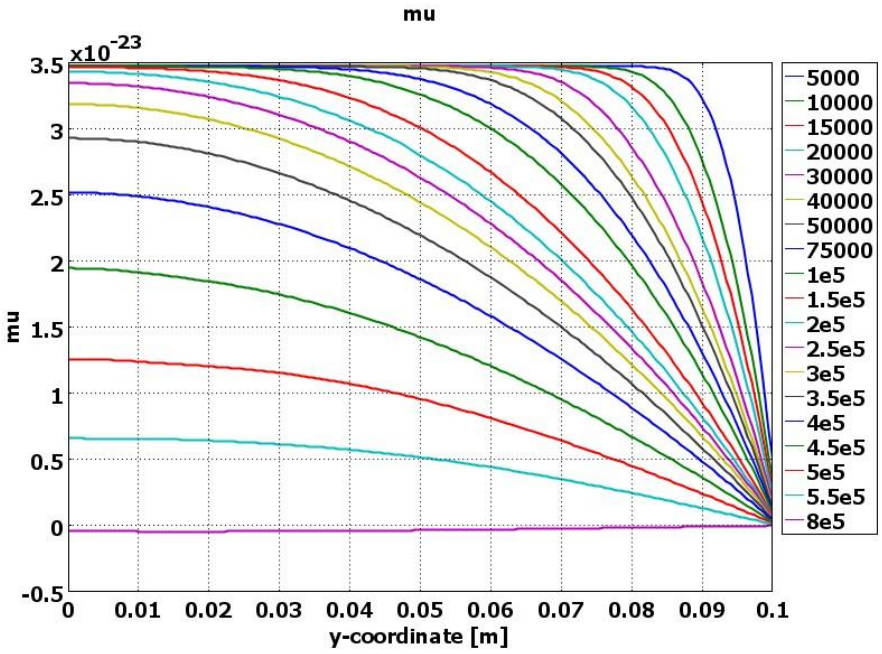

Figure 29. Evolution of the chemical potential in the thickness of the gel

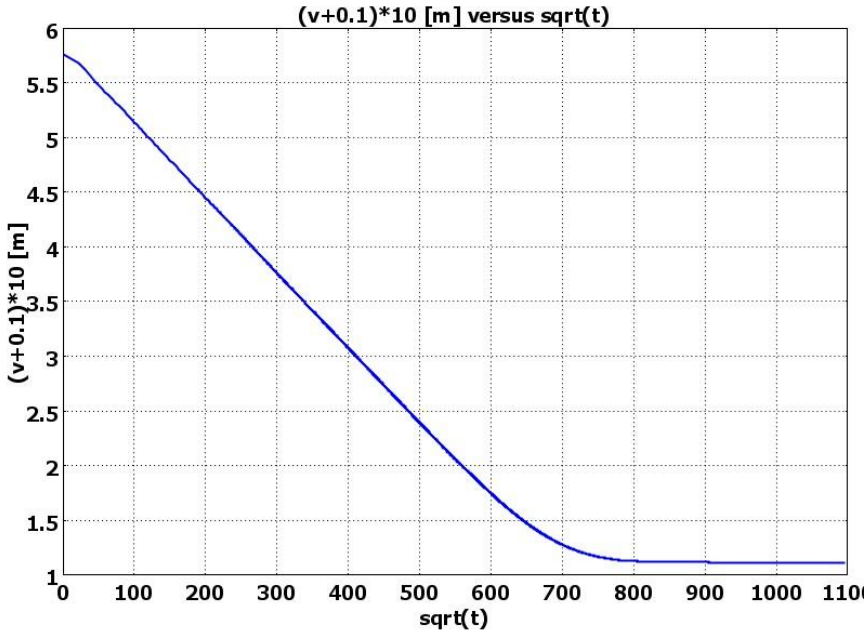

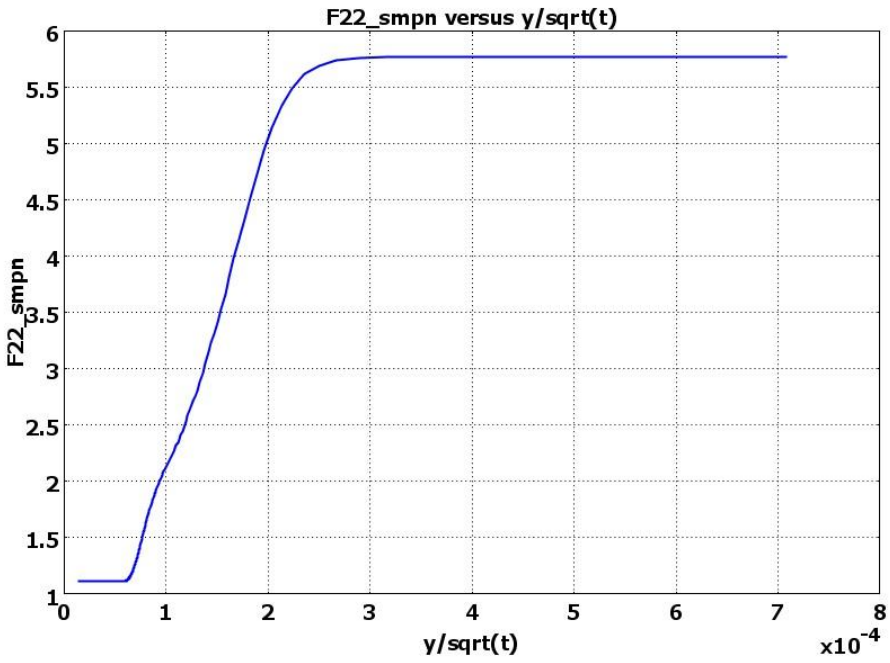

Good results: same as the analytical results

Test with “adimention”: problem with speed flux/diffusion but with “makeshift job” the results are as good as the one in Matlab

Test without “adimention”: with a very fine mesh the results are quite good

III. Creep uniaxial in 3D

Stationary resolution: good final state for any weight

Problem with the transient part: λ_3 is constant in the layer and the same “makeshift job” as in 2D is very unstable, Comsol cannot run a too fine mesh…

Creep uniaxial in 2D starting from swelled state

Problem with creep uniaxial 3D

(=>see summary Comsol)

For each example:

- presentation of the example: geometry, CL, cost, mesh
- goal of the example
- discussion: what's working, what's not

Chapter 5 : Discussion/ conclusion

What we've done

(1. What's working

2. What's not

3. Improvements)

A. Propositions of explanations on the failed case

Why "adimention" is necessary:

- too slow diffusion does not enter the first element?

- …

Why we cannot get good results in the creep uniaxial test in 2D without "makeshift job"?

-the modelisation of the flux gives a too slow one compared to the diffusion characteristic time?

- the adimentionalisation is so good?

- ….

Why is it so long to swell?

- because of the expression of the flux linearly dependent on μ?

-…

Why we cannot get instatbility for the transient part in the creep uniaxial test in 3D?

- problem of choc with the pressure, μ?

- a very fine mesh(too many dofs) is necessary because of the thin front

-…

B. Feasible improvements

Change in some hypothesis

Monophasic theory -> biphasic theory

Hypothesis of incompressibility

….

Conclusion

(to include in the last part ?)

idée directrice

what was the purpose

quick summary of the steps of the project

what was possible, percepective

References

Biot, M.A., 1941. General theory of three-dimensional consolidation. J. Appl. Phys. 12 (2), 155–164.

Bromberg, L. E., Ron, E. S., 1998. Temperature-responsive gels and thermogelling polymer matrices for protein and peptide delivery. Advanced Drug Delivery Reviews 31 (1998) 197-221

De Kee, D., Liu, Q. and Hinestroza , 2005. Viscoelastic (non-fickian) diffusion, Canadian Journal of Chemical Engineering. 83(6): 913-929

Detournay, E., Cheng, A.H.-D., 1993. Fundamentals of poroelasticity. In: Hudson, J.A. (Ed.), Comprehensive Rock Engineering: Principles, Practices and Projects, vol. 2. Pergamon Press, Oxford, UK, pp. 113–171.

Dolbow, J., Fried, E., Ji, H., 2005. A numerical strategy for investigating the kinetic response of stimulus-responsive hydrogels. Comput.

Dolbow, J., Fried, E., Jia, H.D., 2004. Chemically induced swelling of hydrogels. J. Mech. Phys. Solids 52 (1), 51–84.

Durning, C.J., Morman, K.N., 1993. Nonlinear swelling of polymer gels. J. Chem. Phys. 98 (5), 4275–4293.

Durning, C.J., Morman, K.N., 1993. Nonlinear swelling of polymer gels. J. Chem. Phys. 98 (5), 4275–4293.

Feynman, R.P., Leighton, R.B., Sands, M., 1963. The Feynman Lectures on Physics. p. I-43-9.

Flory, P. J., 1977. J. Chem. Phys. 66, 5720

Flory, P.J., Rehner, J., 1943. Statistical mechanics of cross-linked polymer networks. II. Swelling. J. Chem. Phys. 11 (11), 521–526.

Gao, Y.C., 1999. A special mechanical behavior of gels and its micro mechanism. doi: 10. 1016/S0093-6413(00)00083-5

Gibbs, J.W., 1878. The Scientific Papers of J. Willard Gibbs. pp. 184, 201, 215. Digital copy of the book is freely available at < /http://books.google.com/>.

Hong, W., 2007. A theory of coupled diffusion and large deformation in polymeric gels**,** </http://imechanica.org/1926>.

Hong, W., Zhao, X., Zhou, J., Suo, Z., 2008a. A theory of coupled diffusion and large deformation in polymeric gels. J. Mech. Phys. Solids, doi: 10.1016/j.jmps.2007.11.010

Hong, W., Liu, Z., Suo, Z., 2008b. Inhomogeneous swelling of a gel in equilibrium with a solvent and mechanical load, submitted for publication.

Horkay, F., McKenna, G.B., 2007. Polymer networks and gels. In: Mark, J.E. (Ed.), Physical Properties of Polymers Handbook. Springer, New York, pp. 497–523.

Jiang, H., 2008. A Finite Element Method for Transient Analysis of Concurrent Large Deformation and Mass Transport in Gels </http://imechanica.org/node/3895>

Kausch, H.H., Heymans, N., Plummer, C.J., Decroly, P., 2001. Traité des matériaux Volume 14 Matériaux polymères : Propriétés mécaniques et physiques Principe de mise en oeuvre, Presse Polytechniques et Universitaires Romanes, p56-59, p85-87

Qi, H.J., 2007. The mechanics of hydrogel.< /http://imechanica.org/node/1641>

Qiu, Y., Park, K., 2001. Environment-sensitive hydrogels for drug delivery. Advanced Drug Delivery Reviews 53 (2001) 321-339

Rice, J.R., 1998. Elasticity of Fluid-Infiltrated Porous Solids (Poroelasticity) , notes for teaching on hydrology and environmental geomechanics

Rice, J.R., Cleary, M.P., 1976. Some basic stress diffusion solutions for fluid-saturated elastic porous-media with compressible constituents. Rev. Geophys. 14 (2), 227–241.

Ronca, G., Allegra, 1975. J. Chem. Phys. 63, 4990 (1975)

Suo, Z., 2007. Poroelasticity, or diffusion in an elastic solid. < /http://imechanica.org/node/987>.

Suo, Z., 2008. Large deformation and instability in gels, slides of a talk in the Schlumberger-Doll Research Center.

Suo, Z., 2008. Large deformation and instability in gels. < /http://imechanica.org/node/2789>.

Tanaka, T., Fillmore, D.J., 1979. Kinetics of swelling of gels. J. Chem. Phys. 70 (3), 1214–1218.

Tanaka, T., Hocker, L.O., Benedek, G.B., 1973. Spectrum of light scattered from a viscoelastic gel. J. Chem. Phys. 59 (9), 5151–5159.

Tsai, H., Pence, T.J., Kirkinis, E., 2004. Swelling induced finite strain flexure in a rectangular block of an isotropic elastic material. J. Elasticity 75 (1), 69–89.

Wikipedia, Gel, article

Zhang, Z., Zhao, X., Suo, Z., Jianq, H., 2008. A Finite Element Method for Transient Analysis of Concurrent Large Deformation and Mass Transport in Gels

Appendix

I. Matlab Programs

A. Determination of the free swelling stretches

```
function y=hzero(x)
ksi=0.2;
D=8*(10^-10);
nv=10^-3;
y=(nv/x.^2)*(1-1/x)+ x.^2*log(1-1/(x.^3))+1/(x.^3)+ksi/(x.^6)
```

B. Determination of $\lambda_3(0,t)$ for the creep uniaxial problem

```
function y=hzero2(x)
ksi=0.2;
l1=3.215;
D=8*(10^-10);
nv=10^-3;
cst = -0.05  %sv/kT
y=(l1.^2)*(log(1-1/(x.*(l1.^2)))+1/(x.*(l1.^2))+ksi/(x.^2.*(l1.^4))+(nv/(l1.^2))*(x-1/x))-cst;
```

C. Resolution of the PDE of $\lambda_3(0,t)$ for several times

```
function pdex2 % for different times
m = 0;
x = linspace(0,1,100);
t = linspace(0,2.5000e+11,500);

sol = pdepe(m,@pdex1pde,@pdex1ic,@pdex1bc,x,t);
% Extract the first solution component as u.
u = sol(:,:,1);

% A solution profile can also be illuminating.
figure
plot(x,u(end,:))
title('Solution at different times')
xlabel('Dimensionless reference coordinate X3/L')
ylabel('lambda3(X3,t)')

hold on
```

```
% A solution profile can also be illuminating.
%figure
plot(x,u(200,:))
plot(x,u(100,:))
plot(x,u(50,:))
plot(x,u(20,:))
plot(x,u(5,:))
plot(x,u(2,:))
plot(x,u(1,:))

%long/short time limit
plot(x,3.215)
plot(x,0.8183)

% --------------------------------------------------------------
function [c,f,s] = pdex1pde(x,t,u,DuDx)
ksi=0.2;
l1=3.215;
D=8*(10^-10);
nv=10^-3;
c = 1;
f = D*(1-1/(l1.^2.*u))*(1/((l1.^2.*u-1)*l1.^2.*u.^3)-2*ksi/(l1.^4.*u.^4)+(nv/(l1.^2.*u))*(1+1/u.^2))*DuDx;
s = 0;
% --------------------------------------------------------------
function u0 = pdex1ic(x)
u0 = 3.215;
% --------------------------------------------------------------
function [pl,ql,pr,qr] = pdex1bc(xl,ul,xr,ur,t)
ksi=0.2;
l1=3.215;
D=8*(10^-10);
nv=10^-3;
cst=-0.05;

pl = ul- 0.8183; % (l1.^2)*(log(1-1/(ul.*l1.^2))+1/(ul.*l1.^2)+ksi/(ul.^2*l1.^4)+(nv/l1.^2)*(ul-1/ul))-cst;
ql = 0;
pr = 0;
```

```
qr = 1/(D*(1-1/(l1.^2.*ur))*(1/((l1.^2.*ur-1)*l1.^2.*ur.^3)-
2*ksi/(l1.^4.*ur.^4)+(nv/(l1.^2.*ur))*(1+1/ur.^2)));
```

D. Determination of the thickness evolution for several weights

```
function pdex3 %problem tangent at 0

m = 0;
x = linspace(0,1,100);
t = linspace(0,2.5000e+12,300);
y=sqrt(t*10^-3);

sol = pdepe(m,@pdex1pde,@pdex1ic,@pdex1bc,x,t);
% Extract the first solution component as u.
u = sol(:,:,1);

sol2 = pdepe(m,@pdex1pde,@pdex1ic,@pdex2bc,x,t);
u2 = sol2(:,:,1);

sol3 = pdepe(m,@pdex1pde,@pdex1ic,@pdex3bc,x,t);
u3 = sol3(:,:,1);

sol4 = pdepe(m,@pdex1pde,@pdex1ic,@pdex4bc,x,t);
u4 = sol4(:,:,1);

% Computation of the thickness of the gel
for i=1:300
uu = sol(i,:,1);
tru(i) = trapz (x,uu);  % create a vector with the thickness of the gel
end

for i=1:300
uu = sol2(i,:,1);
tru2(i) = trapz (x,uu);
end

for i=1:300
uu = sol3(i,:,1);
tru3(i) = trapz (x,uu);
```

```
end

for i=1:300
uu = sol4(i,:,1);
tru4(i) = trapz (x,uu);
end

% A solution profile can also be illuminating.
figure
plot(y,tru)%(:,2))
%axis([0 0.3 0 3.5])
title('Solution for different applied weight')
xlabel('sqrt t')
ylabel('thickness of the gel l/L')
 hold on

plot(y,tru2)
plot(y,tru3)
plot(y,tru4)

% --------------------------------------------------------------
function [c,f,s] = pdex1pde(x,t,u,DuDx)
ksi=0.2;
l1=3.215;
D=8*(10^-10);
nv=10^-3;
c = 1;
f = D*(1-1/(l1.^2.*u))*(1/((l1.^2.*u-1)*l1.^2.*u.^3)-2*ksi/(l1.^4.*u.^4)+(nv/(l1.^2.*u))*(1+1/u.^2))*DuDx;
s = 0;
% --------------------------------------------------------------
function u0 = pdex1ic(x)
u0 = 3.215;
% --------------------------------------------------------------

%sv/kt=-0.05
function [pl,ql,pr,qr] = pdex1bc(xl,ul,xr,ur,t)
ksi=0.2;
l1=3.215;
D=8*(10^-10);
```

```
nv=10^-3;
cst=-0.03;

pl = ul- 0.8183; % (l1.^2)*(log(1-1/(ul.*l1.^2))+1/(ul.*l1.^2)+ksi/(ul.^2*l1.^4)+(nv/l1.^2)*(ul-1/ul))-cst;
ql = 0;
pr = 0;
qr = 1/(D*(1-1/(l1.^2.*ur))*(1/((l1.^2.*ur-1)*l1.^2.*ur.^3)-
2*ksi/(l1.^4.*ur.^4)+(nv/(l1.^2.*ur))*(1+1/ur.^2)));

%sv/kt=-0.03
function [pl,ql,pr,qr] = pdex2bc(xl,ul,xr,ur,t)
ksi=0.2;
l1=3.215;
D=8*(10^-10);
nv=10^-3;
cst=-0.05;

pl = ul- 1.0358; % (l1.^2)*(log(1-1/(ul.*l1.^2))+1/(ul.*l1.^2)+ksi/(ul.^2*l1.^4)+(nv/l1.^2)*(ul-1/ul))-cst;
ql = 0;
pr = 0;
qr = 1/(D*(1-1/(l1.^2.*ur))*(1/((l1.^2.*ur-1)*l1.^2.*ur.^3)-
2*ksi/(l1.^4.*ur.^4)+(nv/(l1.^2.*ur))*(1+1/ur.^2)));

%sv/kt=-0.1
function [pl,ql,pr,qr] = pdex3bc(xl,ul,xr,ur,t) %sv/kt=-0.05
ksi=0.2;
l1=3.215;
D=8*(10^-10);
nv=10^-3;
cst=-0.1;

pl = ul- 0.5949; % (l1.^2)*(log(1-1/(ul.*l1.^2))+1/(ul.*l1.^2)+ksi/(ul.^2*l1.^4)+(nv/l1.^2)*(ul-1/ul))-cst;
ql = 0;
pr = 0;
qr = 1/(D*(1-1/(l1.^2.*ur))*(1/((l1.^2.*ur-1)*l1.^2.*ur.^3)-
2*ksi/(l1.^4.*ur.^4)+(nv/(l1.^2.*ur))*(1+1/ur.^2)));

%sv/kt=-0.2
function [pl,ql,pr,qr] = pdex4bc(xl,ul,xr,ur,t)
```

```
ksi=0.2;
l1=3.125;
D=8*(10^-10);
nv=10^-3;
cst=-0.2;

pl = ul- 0.4358; % (l1.^2)*(log(1-1/(ul.*l1.^2))+1/(ul.*l1.^2)+ksi/(ul.^2*l1.^4)+(nv/l1.^2)*(ul-1/ul))-cst;
ql = 0;
pr = 0;
qr = 1/(D*(1-1/(l1.^2.*ur))*(1/((l1.^2.*ur-1)*l1.^2.*ur.^3)-
2*ksi/(l1.^4.*ur.^4)+(nv/(l1.^2.*ur))*(1+1/ur.^2)));
```

E. Resolution of self-similar ODE

```
function selfsimilar2

x= linspace (0,0.2,40);

 para=0;
solinit= bvpinit (x, @ssinit,para);   %para=parameter use only to had a condition

  sol = bvp4c(@ssode,@ssbc,solinit);

   xint=linspace (0,0.2);
   Sxint = deval(sol,xint,1);
   figure
   plot(xint,Sxint(1,:))
   title('Self-similar equation.')
   xlabel('x')
   ylabel('solution y')

   sol2 = bvp4c(@ssode,@ssbc2,solinit);
   sol3 = bvp4c(@ssode,@ssbc3,solinit);
   sol4 = bvp4c(@ssode,@ssbc4,solinit);

   hold on
   Sxint2 = deval(sol2,xint);
   Sxint3 = deval(sol3,xint);
   Sxint4 = deval(sol4,xint);
   plot(xint,Sxint2(1,:))
```

```
    plot(xint,Sxint3(1,:))
    plot(xint,Sxint4(1,:))

 %-------------------------------------------------------------------------
%for light weight
function dydt = ssode(x,y,para)  %ODE
ksi=0.2;
l1=3.125;
nv=10^-3;

dydt = [y(2)
    para+(-(x/2)*y(2) - (-4/(l1^4*y(1)^5)+2*ksi*(4*l1^2*y(1)-5)/(l1^6*y(1)^6)+(nv/(l1.^4.*y(1)^5))*(4-
3*l1^2*y(1)+2*y(1)^2-l1^2*y(1)^3))* y(2)^2) / ((1-1/(l1.^2.*y(1)))*(1/((l1.^2.*y(1)-1)*l1.^2.*y(1).^3)  -
2*ksi/(l1.^4.*y(1).^4)+(nv/(l1.^2.*y(1)))*(1+1/y(1).^2))) ];
%-------------------------------------------------------------------------

function res = ssbc(ya,yb,para) %BC
lambda=fzero(@hzer,2);
res = [     ya(1)-lambda
          yb(1)-3.215 %];
         yb(2) ];

%-------------------------------------------------------------------------
function yinit = ssinit(x)  %initial guess
yinit = [ 2.1393  % + x^2   + 5.3785*x
        0.2]; %x^2-x+

%-------------------------------------------------------------------------
%-------------------------------------------------------------------------
function res = ssbc2(ya,yb,para)
lambda=fzero(@hzer2,2);
res = [     ya(1)-lambda
          yb(1)-3.215 %];
         yb(2) ];
 %-------------------------------------------------------------------------
function res = ssbc3(ya,yb,para)
lambda=fzero(@hzer3,2);
res = [     ya(1)-lambda
          yb(1)-3.215 %];
```

```
        yb(2) ];
 %-----------------------------------------------------------------------
function res = ssbc4(ya,yb,para)
lambda=fzero(@hzer4,2);
res = [     ya(1)-lambda
         yb(1)-3.215 %];
        yb(2) ];

%-----------------------------------------------------------------------
function y=hzero(x,cst)
ksi=0.2;
l1=3.215;
D=8*(10^-10);
nv=10^-3;
%cst=-0.005;

y=(l1.^2)*(log(1-1/(x.*(l1.^2)))+1/(x.*(l1.^2))+ksi/(x.^2.*(l1.^4))+(nv/(l1.^2))*(x-1/x))-cst;
%-----------------------------------------------------------------------
function y2=hzer(x)
y2=hzero(x,-0.01);
%-----------------------------------------------------------------------
function y2=hzer2(x)
y2=hzero(x,-0.05);
%-----------------------------------------------------------------------
function y2=hzer3(x)
y2=hzero(x,-0.1);
%-----------------------------------------------------------------------
function y2=hzer4(x)
y2=hzero(x,-0.2);
```

II. Variables in COMSOL Multiphysics

A. Constants

NkT3D	4e4[N/m^2]	constant1 for Flory-Rehner 3D
NkT2D	1.1587e4[N/m^2]	constant1 for Flory-Rehner 2D
kTonv	4e7[Pa]	constant2 for Flory-Rehner
ksi	0.2	dimensionless measure of enthalpy of mixing
vol	6.022e-5[m^3/mol]	volume per mole of molecule
D1tt	8e-10[m^2/s]	coefficient of diffusion of particules
kT	4e-21[J]	constant for mu
volm3	1e-28[m^3]	volume per molecule
D1	8e-1[m^2/s]	dimensionless diffusion coefficient
Ce1	5.3522[mol/m^3]	dimensionless external concentration
ceps1	1[mol/m^3]	

B. Scalar expressions for 2D models

d11	(D1/(1+vol*c)^2)*(1-2*ksi*vol*c/(1+vol*c)) *(invF11_smpn^2+invF12_smpn^2)	coefficient of diffusion 11
d12	(D1/(1+vol*c)^2)*(1-2*ksi*vol*c/(1+vol*c)) * (invF11_smpn*invF21_smpn+invF12_smpn*invF22_smpn)	coefficient of diffusion 12
d21	d12	coefficient of diffusion 21
d22	(D1/(1+vol*c)^2)*(1-2*ksi*vol*c/(1+vol*c)) *(invF22_smpn^2+invF21_smpn^2)	coefficient of diffusion 22
Ws_smpn_diff	(0.5*NkT*(-3+I1_smpn-log(I3_smpn))- kTonv*(vol*c*log(1+1/(vol*c)) +ksi/(1+vol*c)) -p*(-1+Jel_smpn-vol*c+0.5*p/kappa_smpn))*thickness_smpn	total strain energy
Ws_smpn_diff1	(-kTonv*(vol*c*log(1+1/(vol*c))+ksi/(1+vol*c)) -p*(-1+Jel_smpn-vol*c+0.5*p/kappa_smpn))*thickness_smpn	diffusion strain energy
mup	kT*(log(vol*c2/(1+vol*c2))+1/(1+vol*c2)+ksi/(1+vol*c2)^2)+p*volm3	
ceps	ceps1*(1[s]-t*0.1)*(t<10)	
C2	c*10^5	dimensionless concentration

C. Scalar expressions for 3D models

d11	(D1/(1+vol*c)^2)*(1-2*ksi*vol*c/(1+vol*c)) *(invF11_smsld^2+invF12_smsld^2+invF13_smsld^2)	coefficient of diffusion 11
d22	(D1/(1+vol*c)^2)*(1-2*ksi*vol*c/(1+vol*c)) *(invF21_smsld^2+invF22_smsld^2+invF23_smsld^2)	coefficient of diffusion 22
d33	(D1/(1+vol*c)^2)*(1-2*ksi*vol*c/(1+vol*c)) *(invF31_smsld^2+invF32_smsld^2+invF33_smsld^2)	

d12	(D1/(1+vol*c)^2)*(1-2*ksi*vol*c/(1+vol*c)) *(invF11_smsld*invF21_smsld+invF12_smsld*invF22_smsld +invF13_smsld*invF23_smsld)	coefficient of diffusion 12
d13	(D1/(1+vol*c)^2)*(1-2*ksi*vol*c/(1+vol*c)) *(invF11_smsld*invF31_smsld+invF12_smsld*invF32_smsld +invF13_smsld*invF33_smsld)	coefficient of diffusion 21
d23	(D1/(1+vol*c)^2)*(1-2*ksi*vol*c/(1+vol*c)) *(invF21_smsld*invF31_smsld+invF22_smsld*invF32_smsld +invF23_smsld*invF33_smsld)	
Ws_smsld_2	(0.5*NkT*(-3+I1_smsld-log(I3_smsld))- kTonv*(vol*c2*log(1+1/(vol*c2)) +ksi/(1+vol*c2))-p*(-1+Jel_smsld-vol*c2+p/kappa_smsld))	total strain energy
Ws_smpn_diff1	(-kTonv*(vol*c2*log(1+1/(vol*c2))+ksi/(1+vol*c2)) -p*(-1+Jel_smsld-vol*c2+0.5*p/kappa_smsld))	diffusion strain energy
mup	kT*(log(vol*c2/(1+vol*c2))+1/(1+vol*c2)+ksi/(1+vol*c2)^2)+p*volm3	chemical potential
Ce	Ce1*0.5*(1+tanh(2[s^-1]*(t-2.5[s])))	
c2	c*10^5	
ceps	ceps1*(1[s]-t*0.1)*(t<10)	